

Strong decays analysis of excited nonstrange charmed mesons: Implications for spectroscopy

Keval Gandhi* and Ajay Kumar Rai†

*Department of Applied Physics,
Sardar Vallabhbhai National Institute of Technology,
Surat 395007, Gujarat, India.*

(Dated: November 27, 2019)

The strong decays of $D_1(2420)^0$, $D_2^*(2460)^0$, $D_2^*(2460)^+$, $D_2^*(2460)^-$, $D(2550)^0$, $D_J^*(2600)^0$, $D(2740)^0$, $D_3^*(2750)^0$, $D_3^*(2750)^+$, $D_3^*(2750)^-$, $D_J(3000)^0$, $D_J^*(3000)^0$ and $D_2^*(3000)^0$ resonance states are analyzed in the heavy quark mass limit of Heavy Quark Effective Theory (HQET). The individual decay rates and the branching ratios among the strong decays determine their spin and parity. From such states the Regge trajectories are constructed in (J, M^2) and (n_r, M^2) planes and further predict the masses of higher excited states (1^1D_2 , 1^3D_3 , 3^1S_0 , 3^3S_1 , 1^1F_3 , 1^3F_4 , 2^3D_3 , 3^3P_2 and 2^3F_4) lying on Regge lines by fixing their slopes and intercepts. Moreover, the strong decay rates and the branching ratios of these higher excited states are also examined, which can help the experimentalists to search these states into their respective decay modes.

I. INTRODUCTION

Remarkable progress has been made in the field of charmed meson spectroscopy recently by experimental observations as well as theoretical computations. Different experimental facilities have provided new informations in this sector like masses, decay widths, branching ratios, isospin mass splittings, spin, parity, polarization amplitude etc.. At latest, the LHCb Collaboration has studied the amplitude contribution in $B^- \rightarrow D^+ \pi^- \pi^-$ decay using the Dalitz plot analysis technique [1]. They found that the main contributions are coming from the $D_2^*(2460)^0$, $D_1^*(2680)^0$, $D_3^*(2760)^0$ and $D_2^*(3000)^0$ resonances which are decaying into S -wave $D^+ \pi^-$. Their masses and decay widths are measured precisely (with statistical and systematic uncertainties) and make a spin parity assignment of $D_2^*(3000)^0$ as 2^+ first time. The LHCb group in their earlier analysis of decay $B^0 \rightarrow \bar{D}^0 \pi^+ \pi^-$ has measured $D_0^*(2400)^-$ and $D_0^*(2460)^-$ mesons and identified the $D_3^*(2760)^-$ with a spin parity 3^- in the squared invariant mass region of $\bar{D}^0 \pi^-$ [2].

In 2013, the LHCb detector found $D^+ \pi^-$, $D^0 \pi^+$ and $D^{*+} \pi^-$ final state mass spectra at the centre-of-mass energy 7 TeV of pp collision [3]. They have observed the rich spectrum of nonstrange charmed mesons, $D_J^*(2580)^0$ and $D_0^*(2740)^0$ with unnatural parity ($0^-, 1^+, 2^-$, ...) in the $D^{*+} \pi^-$ decay mode. The mass spectra analysis of $D^+ \pi^-$, $D^0 \pi^+$ and $D^{*+} \pi^-$ reconstruct the masses and the decay widths of $D_2^*(2460)$. The $D_J^*(2650)^0$ and $D_J^*(2760)^0$ are found with the natural parity ($0^+, 1^-, 2^+$, ...) in the $D^{*+} \pi^-$ mass spectra. Along with these they have also got the resonant structures in a region around 3 GeV. The $D_J(3000)^0$ was observed in $D^{*+} \pi^-$ decay mode with unnatural parity and the $D_J^*(3000)^0$ in $D^+ \pi^-$ with natural parity [3].

Earlier, the *BABAR* experiment had collected the data sample of excited D mesons resonances corresponding to an integrated luminosity 454 fb^{-1} of e^+e^- collision at the center-of-mass energy 10.58 GeV [4]. The masses and decay widths of the observed D mesons ($D(2550)^0$, $D^*(2600)^0/+$, $D(2750)^0$ and $D^*(2760)^0/+$), are reconstructed from $D^+ \pi^-$, $D^0 \pi^+$ and $D^{*+} \pi^-$ decay resonances. Moreover, the helicity distribution analysis identified $D(2550)^0$ and $D^*(2600)^0$ as a $2S$ doublet of spin-parity 0^- and 1^- respectively; and the states $D(2750)^0$ and $D^*(2760)^0/+$ belong to $L = 2$ (L is the orbital angular momentum). The masses, decay widths, spin-parity observed by the experimental groups LHCb [1–3] and the *BABAR* [4] are presented in Table I with their respective observed decay modes.

Experimentally, the Dalitz plot model in the B decay production determines the spin-parity and the prompt production analysis differentiate the hadrons with natural and unnatural parity. Moreover, the ratio of the branching fractions measurement of strong decay modes can help to classify the decaying mesons. It is very crucial to assign the spin-parity of hadrons which facilitate the determination of experimental properties. According to the latest Review of Particle Physics (RPP) by Particle Data Group (PDG), the J^P (J is the total spin and P is parity) values of $D_1(2420)^{\pm}$, $D(2550)^0$, $D_J^*(2600)$, $D^*(2640)^{\pm}$, $D(2740)^0$ and $D(3000)^0$ mesons are not yet confirmed from the known experimental measurements [5]. Many theoretical groups have computed the excited state masses of charmed mesons with the help of various potential models. Recently, Jiao-Kai Chen obtained the radial and orbital Regge trajectories by applying the Bohr-Sommerfeld quantization approach [6]. Other variants include semi-relativistic approach [7], Godfrey-Isgur (GI) relativized quark model [8], relativistic quark model [9], Lakhina and Swanson proposed nonrelativistic constituent quark model [10], the Quantum Chromodynamics (QCD) motivated relativistic quark model based on the quasipotential approach [11], relativistic quark model

* keval.physics@yahoo.com

† raiajayk@gmail.com

TABLE I. The experimental results (masses and decay widths) from LHCb(2016) [1], LHCb(2015) [2], LHCb(2013) [3] and *BABAR*(2010) [4] of nonstrange charmed mesons (in MeV).

Meson	LHCb(2016) [1]	LHCb(2015) [2]	LHCb(2013) [3]	<i>BABAR</i> (2010) [4]	Decay mode
$D_1(2420)^0$			$2419.6 \pm 0.1 \pm 0.7$ $35.2 \pm 0.4 \pm 0.9$ 1^+	$2420.1 \pm 0.1 \pm 0.8$ $31.4 \pm 0.5 \pm 1.3$ Unnatural	$D^{*+}\pi^-$
$D_2^*(2460)^0$	$2463.7 \pm 0.4 \pm 0.4 \pm 0.6$ $47.0 \pm 0.8 \pm 0.9 \pm 0.3$ 2^+		$2460.4 \pm 0.1 \pm 0.1$ $45.6 \pm 0.4 \pm 1.1$ 2^+	$2462.2 \pm 0.1 \pm 0.8$ $50.5 \pm 0.6 \pm 0.7$ Natural	$D^+\pi^-$
$D_2^*(2460)^+$			$2463.1 \pm 0.2 \pm 0.6$ $48.6 \pm 1.3 \pm 1.9$ 2^+		$D^0\pi^+$
$D_2^*(2460)^-$		$2468.6 \pm 0.6 \pm 0.3$ $47.3 \pm 1.5 \pm 0.7$ 2^+			$D^0\pi^-$
$D(2550)^0$			$2579.5 \pm 3.4 \pm 5.5$ $177.5 \pm 17.8 \pm 46.0$ Unnatural	$2539.4 \pm 4.5 \pm 6.8$ $130 \pm 12 \pm 13$ 0^-	$D^{*+}\pi^-$
$D_J^*(2600)^0$	$2681.1 \pm 5.6 \pm 4.9 \pm 13.1$ $186.7 \pm 8.5 \pm 8.6 \pm 8.2$ 1^-			$2608.7 \pm 2.4 \pm 2.5$ $93 \pm 6 \pm 13$ Natural	$D^+\pi^-$
			$2649.2 \pm 3.5 \pm 3.5$ $140.2 \pm 17.1 \pm 18.6$ Natural		$D^{*+}\pi^-$
$D(2740)^0$			$2737.0 \pm 3.5 \pm 11.2$ $73.2 \pm 13.4 \pm 25.0$ Unnatural		$D^{*+}\pi^-$
$D_3^*(2750)^0$	$2775.5 \pm 4.5 \pm 4.5 \pm 4.7$ $95.3 \pm 9.6 \pm 7.9 \pm 33.1$ 3^-		$2760.1 \pm 1.1 \pm 3.7$ $74.4 \pm 3.4 \pm 19.1$ Natural	$2763.3 \pm 2.3 \pm 2.3$ $60.9 \pm 5.1 \pm 3.6$ Natural	$D^+\pi^-$
			$2761.1 \pm 5.1 \pm 6.5$ $74.4 \pm 3.4 \pm 37.0$ Natural	$2752.4 \pm 1.7 \pm 2.7$ $71 \pm 6 \pm 11$ Natural	$D^{*+}\pi^-$
$D_3^*(2750)^+$			$2771.7 \pm 1.7 \pm 3.8$ $66.7 \pm 6.6 \pm 10.5$ 3^-	$2769.7 \pm 3.8 \pm 1.5$ 60.9 Natural	$D^0\pi^+$
$D_3^*(2750)^-$		$2798 \pm 7 \pm 1 \pm 7$ $105 \pm 18 \pm 6 \pm 23$ 3^-			$D^0\pi^-$
$D_J(3000)^0$				2971.8 ± 8.7 188.1 ± 44.8 Unnatural	$D^{*+}\pi^-$
$D_J^*(3000)^0$				3008.1 ± 4.0 110.5 ± 11.5 Natural	$D^+\pi^-$
$D_2^*(3000)^0$	$3214 \pm 29 \pm 33 \pm 36$ $186 \pm 38 \pm 34 \pm 63$ 2^+				$D^+\pi^-$

TABLE II. Spectra of nonstrange charmed mesons obtained from different models (in MeV).

$\mathcal{N}^{2S+1}L_J$	J^P	Ref. [6]	Ref. [7]	Ref. [8]	Ref. [9]	Ref. [10]	Ref. [11]	Ref. [12]	Ref. [13]	Ref. [14]
1^1S_0	0^-	1869	1884	1877	1874	1867	1871	1868	1874	1865
1^3S_1	1^-	2002	2010	2041	2038	2010	2010	2005	2006	2027
2^1S_0	0^-	2562	2582	2581	2583	2555	2581	2589	2540	
2^3S_1	1^-	2616	2655	2643	2645	2636	2632	2692	2601	
3^1S_0	0^-	2970	3186	3110	3068		3062	3141	2904	
3^3S_1	1^-	3004	3239	3068	3111		3096	3226	2947	
1^3P_0	0^+	2319	2357	2399	2398	2252	2406	2377	2341	2325
1^1P_1	1^+	2411	2425	2456	2457	2402	2426	2417	2389	2468
1^3P_1	1^+	2427	2447	2467	2465	2417	2469	2490	2407	2631
1^3P_2	2^+	2456	2461	2502	2501	2466	2460	2460	2477	2743
2^3P_0	0^+		2976	2931	2932	2752	2919	2949	2758	
2^1P_1	1^+		3016	2924	2933	2866	2932	2995	2792	
2^3P_1	1^+		3034	2961	2952	2926	3021	3045	2802	
2^3P_2	2^+	2893	3039	2957	2957	2971	3012	3035	2860	
3^3P_0	0^+		3536	3343			3346		3050	
3^1P_1	1^+		3567	3328			3365		3082	
3^3P_1	1^+		3582	3360			3461		3085	
3^3P_2	2^+	3214	3584	3353			3407		3142	
1^3D_1	1^-	2775	2755	2817	2816	2740	2788	2795	2750	
1^1D_2	2^-	2789	2754	2816	2827	2693	2806	2775	2639	
1^3D_2	2^-	2737	2783	2845	2834	2789	2850	2833	2727	
1^3D_3	3^-	2796	2788	2833	2833	2719	2863	2799	2633	
2^3D_1	1^-		3315	3231	3231	3.168	3228		3052	
2^1D_2	2^-		3318	3212	3225	3.145	3259		2997	
2^3D_2	2^-		3341	3248	3235	3.215	3307		3029	
2^3D_3	3^-		3355	3226	3226	3.170	3335		2999	
1^3F_2	2^+	3105		3132	3132		3090	3091		
1^1F_3	3^+	3087		3108	3123		3129	3074		
1^3F_3	3^+	2998		3143	3129		3145	3123		
1^3F_4	4^+	3073		3132	3113		3187	3101		

including the leading order corrections in $1/m$ [12], the Blankenbecler-Sugar equation in the framework of heavy-light interaction models [13], the lattice QCD [14] etc..

We summarize the predicted mass spectra in Table II (the symbol $\mathcal{N}^{2S+1}L_J$ is used to represent the meson quantum state; where \mathcal{N} , L and S denote the radial, orbital and the intrinsic spin quantum number respectively). Here, we take their comparison with experimental data and make following conclusions,

- i. Two $1S$ states (D and D^*) and the four $1P$ states ($D_0^*(2300)$, $D_1(2420)$, $D_1(2430)$ and $D_2^*(2460)$) are well established with their respective J^P values.
- ii. $D(2550)^0$ was observed by experimental groups LHCb [3] and *BABAR* [4]. They both suggested that such a state has unnatural parity (but the PDG-2018 [5] need more confirmation). The theoretical studies identified its quantum state 2^1S_0 .
- iii. $D_J^*(2600)^0$ and $D^*(2640)^0$ are probably the same state. From LHCb [3] and *BABAR* [4] its J^P value is consistent with natural parity and it can be a candidate of 2^3S_1 .
- iv. $D(2740)^0$ was observed in a single experiment LHCb [3] with unnatural parity and it can be a candidate of 1^1D_2 or 1^3D_2 state.
- v. $D_3^*(2750)$ belongs to 1^3D_3 quantum state. Experimentally, the LHCb [2] determined its J^P value 3^- . Yet the state $D_1^*(2750)$ is not observed experimentally.
- vi. So far the nature of $D_J(3000)^0$, $D_J^*(3000)^0$ and $D_2^*(3000)^0$ mesons are unsolved theoretically. According to LHCb [3] the $D_J(3000)^0$ has unnatural parity. So it can be a candidate of 3^1S_0 and 2^3P_1 states. $D_J^*(3000)^0$ has natural parity and may belongs to 3^3S_1 , 2^3P_2 , 1^3F_2 and 1^3F_4 quantum states. The LHCb [1] measured the spin parity of $D_2^*(3000)^0$ as 2^+ and can belongs to quantum states 3^3P_2 and 1^3F_2 .

In Ref. [8], S. Godfrey and K. Moats are used 3P_0 quark-pair-creation (QPC) model, and identified $D_J(2550)^0$, $D_J^*(2600)^0$, $D_1^*(2760)^0$, $D_3^*(2760)^-$, $D_J(2750)^0$, $D_J(3000)^0$, and $D_J^*(3000)^0$ states as 2^1S_0 , 2^3S_1 , 1^3D_1 , 1^3D_3 , $1D_2$, 3^1S_0 , and 1^3F_4 respectively; through their strong decays analysis. Y. Sun *et al.* [9] calculate the strong decays of $3S$, $2P$, $2D$, and $1F$ states of D mesons in the 3P_0 QPC model. They assigned $D_J(3000)^0$ and $D_J^*(3000)^0$ as $2P(J^P = 1^+)$ and 2^3P_0 respectively. Also, the Ref. [10] used the same model and examined: $D(2550)$ as 2^1S_0 , $D(2750)$ (or $D(2760)$) as 1^3D_3 state, and the state $D(2600)$ identify as the low-mass mixing of $1^3D_1 - 2^3S_1$ states. Refs. [15, 16] are determined the strong decay rates of excited heavy-light mesons in the chiral constituent quark model. They predict $D(2760)$ as 1^3D_3 and $D_J^*(3000)^0$ as 1^3F_4 , and

$D(2600)$, $D(2750)$ and $D_J(3000)^0$ are found to be a mixed state of $1^3D_1 - 2^3S_1$, $1^1D_2 - 1^3D_1$ and $2^1P_1 - 2^3P_1$ states respectively.

In this work, we analyze the strong decays of excited nonstrange charmed mesons observed by LHCb [1–3] and *BABAR* [4] Collaborations using the Heavy Quark Effective Theory (HQET) in the leading order approximations. On the basis of the strong decay widths and the branching fractions predictions of $D_1(2420)$, $D(2550)$, $D(2740)$, $D_J(3000)$, and $D_2^*(3000)^0$ and their spin partners $D^*(2640)$, $D_J^*(2600)^0$, $D_3^*(2750)$, and $D_J^*(3000)$ we have assigned their spin and parity. Also, the strong coupling constants are determined by comparing the computed strong decay widths with experimental measurements. Similar kind of studies have been done by [17–26] to identify the higher charmed mesonic states. The spectroscopy of a system containing one light (up (u) or down (d) or strange (s)) and one heavy (charm (c) or bottom (b)) quark provides an excellent base to study the Quantum Chromodynamics (QCD) in the low energy regime. Additionally, our tentative spin-parity assignment of nonstrange charmed mesons allow to construct the Regge trajectory in (J, M^2) and (n_r, M^2) planes, where J is the total spin, n_r is the radial principal quantum number and M^2 is the square of the meson mass. They estimate the masses of 1^1D_2 , 1^3D_3 , 3^1S_0 , 3^3S_1 , 1^1F_3 , 1^3F_4 , 2^3D_3 , 3^3P_2 and 2^3F_4 states. Their strong decay rates and branching fraction studies can guide to the experimentalists for searching them in a respective decay channels.

This paper is arranged as follows: after the introduction, section II is a brief description of HQET used to study the strong decays. Section III presents results and discussion, where we attempt to identify the spin and parity of experimentally known excited nonstrange charmed mesons. In section IV we plot the Regge trajectories in (J, M^2) and (n_r, M^2) planes using the masses from PDG-2018 [5]. Further, we analyzed the strong decay rates and the branching fractions of 1^1D_2 , 1^3D_3 , 3^1S_0 , 3^3S_1 , 1^1F_3 , 1^3F_4 , 2^3D_3 , 3^3P_2 and 2^3F_4 states lying on the Regge lines. Finally, the conclusions are presented in section V.

II. THEORETICAL FRAMEWORK

In the framework of heavy quark effective theory (HQET) the properties of heavy-light mesons can be determined systematically by considering infinite mass of one heavy quark, i.e. $m_Q \rightarrow \infty$ [27]. The heavy quark spin and the flavor symmetry arising from the QCD are demolished in this heavy quark (HQ) mass limit and classify the heavy-light mesons according to the total angular momentum of the light antiquark \vec{s}_l , $\vec{s}_l = \vec{s}_{\bar{q}} + \vec{l}$, where $\vec{s}_{\bar{q}}$ and \vec{l} are the spin and the orbital angular momentum of the light antiquark respectively [27].

Here we discuss the D mesons doublets corresponding to s , p , d and f waves for $l = 0, 1, 2$ and 3 respec-

TABLE III. The strong decay widths of nonstrange charmed mesons with possible quantum state assignments (in MeV).

Meson	$\mathcal{N}^{2S+1}L_J$	Decay mode	LHCb(2016) [1]	LHCb(2015) [2]	LHCb(2013) [3]	BABAR(2010) [4]
$D_1(2420)^0$	1^1P_1	$D^{*+}\pi^-$ $D^{*0}\pi^0$ $D_s^{*+}K^-$ $D^{*0}\eta$ Total h_T			$56.2711h_T^2$ $29.3228h_T^2$ — — $85.5939h_T^2$ 0.641	$56.6228h_T^2$ $29.5040h_T^2$ — — $86.1268h_T^2$ 0.604
$D_2^*(2460)^0$	1^3P_2	$D^+\pi^-$ $D^0\pi^0$ $D_s^+K^-$ $D^0\eta$ $D^{*+}\pi^-$ $D^{*0}\pi^0$ $D_s^{*+}K^-$ $D^{*0}\eta$ Total h_T	$127.978h_T^2$ $66.8656h_T^2$ ≈ 0 — $56.3891h_T^2$ $29.7173h_T^2$ — — $280.95h_T^2$ 0.409		$124.786h_T^2$ $65.2218h_T^2$ ≈ 0 — $54.3938h_T^2$ $28.6838h_T^2$ — — $273.085h_T^2$ 0.409	$126.52h_T^2$ $66.1147h_T^2$ ≈ 0 — $55.4757h_T^2$ $29.2442h_T^2$ — — $277.355h_T^2$ 0.427
$D_2^*(2460)^+$	1^3P_2	$D^0\pi^+$ $D^+\pi^0$ $D_s^+K^0$ $D^+\eta$ $D^{*0}\pi^+$ $D^{*+}\pi^0$ $D_s^{*+}K^0$ $D^{*+}\eta$ Total h_T			$131.875h_T^2$ $63.6968h_T^2$ ≈ 0 — $58.0702h_T^2$ $28.494h_T^2$ — — $282.136h_T^2$ 0.415	
$D_2^*(2460)^-$	1^3P_2	$D^0\pi^-$ $D^-\pi^0$ $D_s^-K^0$ $D^-\eta$ $D^{*0}\pi^-$ $D^{*-}\pi^0$ $D_s^{*-}K^0$ $D^{*-}\eta$ Total h_T		$137.440h_T^2$ $66.4136h_T^2$ ≈ 0 — $61.5865h_T^2$ $30.2238h_T^2$ — — $295.664h_T^2$ 0.400		
$D(2550)^0$	2^1S_0	$D^{*+}\pi^-$ $D^{*0}\pi^0$ $D_s^{*+}K^-$ $D^{*0}\eta$ Total g_H^\dagger			$864.734g_H^{\dagger 2}$ $441.692g_H^{\dagger 2}$ — $3.87486g_H^{\dagger 2}$ $1310.30g_H^{\dagger 2}$ 0.368	$709.405g_H^{\dagger 2}$ $363.314g_H^{\dagger 2}$ — — $1072.72g_H^{\dagger 2}$ 0.348

continued...

tively. For the s wave, $l = 0$ gives $\vec{s}_l^P = \frac{1}{2}^-$, the ground state doublet, which consists of two states represented by (P, P^*) , having $J_{s_l}^P = (0^-, 1^-)_{\frac{1}{2}-}$. For the p wave, $l = 1$, the first orbital excited states have two doublets $\vec{s}_l^P = \frac{1}{2}^+$ and $\vec{s}_l^P = \frac{3}{2}^+$, having $J_{s_l}^P = (0^+, 1^+)_{\frac{1}{2}+}$ and $J_{s_l}^P = (1^+, 2^+)_{\frac{3}{2}+}$ represented by (P_0^*, P_1') and (P_1, P_2^*) respectively. Similarly, for the d wave, $l = 2$, two doublets $\vec{s}_l^P = \frac{3}{2}^-$ and $\vec{s}_l^P = \frac{5}{2}^-$, having $J_{s_l}^P = (1^-, 2^-)_{\frac{3}{2}-}$

and $J_{s_l}^P = (2^-, 3^-)_{\frac{5}{2}-}$ are represented by (P_1^*, P_2) and (P_2', P_3^*) respectively. And, for the f wave, $l = 3$, two doublets $\vec{s}_l^P = \frac{5}{2}^+$ and $\vec{s}_l^P = \frac{7}{2}^+$, having $J_{s_l}^P = (2^+, 3^+)_{\frac{5}{2}+}$ and $J_{s_l}^P = (3^+, 4^+)_{\frac{7}{2}+}$ are represented by (P_2^*, P_3) and (P_3', P_4^*) respectively. The above symbols (P, P^*, \dots) are used for radial quantum number $n = 1$ and the same classifications follows for higher radial excitations ($n = 2, 3, \dots$). For $n = 2$, these symbols are denoted with

TABLE III. The strong decay widths of nonstrange charmed mesons with possible quantum state assignments (in MeV).

Meson	$\mathcal{N}^{2S+1}L_J$	Decay mode	LHCb(2016) [1]	LHCb(2015) [2]	LHCb(2013) [3]	BABAR(2010) [4]
$D_J^*(2600)^0$	2^3S_1	$D^+\pi^-$	$680.382g_H^{\dagger 2}$			$541.421g_H^{\dagger 2}$
		$D^0\pi^0$	$345.515g_H^{\dagger 2}$			$274.992g_H^{\dagger 2}$
		$D_s^+K^-$	$199.173g_H^{\dagger 2}$			$104.757g_H^{\dagger 2}$
		$D^0\eta$	$47.9086g_H^{\dagger 2}$			$29.1069g_H^{\dagger 2}$
		$D^{*+}\pi^-$	$886.679g_H^{\dagger 2}$			$656.589g_H^{\dagger 2}$
		$D^{*0}\pi^0$	$450.689g_H^{\dagger 2}$			$334.839g_H^{\dagger 2}$
		$D_s^{*+}K^-$	$78.3291g_H^{\dagger 2}$			≈ 0
		$D_s^{*0}\eta$	$31.0273g_H^{\dagger 2}$			$8.24532g_H^{\dagger 2}$
		Total	$2719.70g_H^{\dagger 2}$			$1949.95g_H^{\dagger 2}$
		g_H^\dagger	0.262			0.218
$D_J^*(2600)^0$	2^3S_1	$D^{*+}\pi^-$		$781.919g_H^{\dagger 2}$		
		$D^{*0}\pi^0$		$397.965g_H^{\dagger 2}$		
		$D_s^{*+}K^-$		$33.6215g_H^{\dagger 2}$		
		$D^{*0}\eta$		$19.8058g_H^{\dagger 2}$		
		$D^+\pi^-$		$617.246g_H^{\dagger 2}$		
		$D^0\pi^0$		$313.774g_H^{\dagger 2}$		
		$D_s^{*+}K^-$		$155.109g_H^{\dagger 2}$		
		$D^0\eta$		$39.2693g_H^{\dagger 2}$		
		Total		$2358.71g_H^{\dagger 2}$		
		g_H^\dagger	0.244			
$D(2740)^0$	1^3D_2	$D^{*+}\pi^-$			$126.986k_Y^2$	
		$D^{*0}\pi^0$			$65.8248k_Y^2$	
		$D_s^{*+}K^-$			$1.92685k_Y^2$	
		$D^{*0}\eta$			$1.30793k_Y^2$	
		Total			$196.046k_Y^2$	
		k_Y			0.611	
$D_3^*(2750)^0$	1^3D_3	$D^+\pi^-$	$190.520k_Y^2$		$172.087k_Y^2$	$175.794k_Y^2$
		$D^0\pi^0$	$98.5331k_Y^2$		$89.0767k_Y^2$	$90.979k_Y^2$
		$D_s^+K^-$	$20.954k_Y^2$		$17.2091k_Y^2$	$17.9416k_Y^2$
		$D^0\eta$	$7.03403k_Y^2$		$5.94594k_Y^2$	$6.16072k_Y^2$
		$D^{*+}\pi^-$	$99.8604k_Y^2$		$88.0932k_Y^2$	$90.4411k_Y^2$
		$D^{*0}\pi^0$	$51.6265k_Y^2$		$45.5895k_Y^2$	$46.7945k_Y^2$
		$D_s^{*+}K^-$	$2.88624k_Y^2$		$2.01803k_Y^2$	$2.17967k_Y^2$
		$D^{*0}\eta$	$1.53565k_Y^2$		$1.16923k_Y^2$	$1.2393k_Y^2$
		Total	$472.95k_Y^2$		$421.189k_Y^2$	$431.53k_Y^2$
		k_Y	0.449		0.420	0.376
$D_3^*(2750)^0$	1^3D_3	$D^{*+}\pi^-$			$88.8216k_Y^2$	$82.6448k_Y^2$
		$D^{*0}\pi^0$			$45.9633k_Y^2$	$42.7926k_Y^2$
		$D_s^{*+}K^-$			$2.06754k_Y^2$	$1.66585k_Y^2$
		$D^{*0}\eta$			$1.1908k_Y^2$	$1.0128k_Y^2$
		$D^+\pi^-$			$173.239k_Y^2$	$163.424k_Y^2$
		$D^0\pi^0$			$89.6677k_Y^2$	$84.6299k_Y^2$
		$D_s^+K^-$			$17.4355k_Y^2$	$15.5399k_Y^2$
		$D^0\eta$			$6.01244k_Y^2$	$5.45238k_Y^2$
		Total			$424.398k_Y^2$	$397.162k_Y^2$
		k_Y			0.419	0.423

continued...

dagger ($P^\dagger, P^{\dagger*}, \dots$) and for $n = 3$ they are ($P^\ddagger, P^{\ddagger*}, \dots$). Hence, each doublet contains two states (or two spin partners) with total spin $J = s_l \pm \frac{1}{2}$ and parity $P = (-1)^{l+1}$ and can be described by the superfields H_a, S_a, T_a, X_a ,

Y_a, Z_a and R_a , written as [28, 29],

$$H_a = \frac{1+i}{2}[P_{a\mu}^* \gamma^\mu - P_a \gamma_5], \quad (1)$$

TABLE III. The strong decay widths of nonstrange charmed mesons with possible quantum state assignments (in MeV).

Meson	$\mathcal{N}^{2S+1}L_J$	Decay mode	LHCb(2016) [1]	LHCb(2015) [2]	LHCb(2013) [3]	BABAR(2010) [4]
$D_3^*(2750)^+$	1^3D_3	$D^0\pi^+$ $D^+\pi^0$ $D_s^+K^0$ $D^+\eta$ $D^{*0}\pi^+$ $D^{*+}\pi^0$ $D_s^{*+}K^0$ $D^{*+}\eta$ Total k_Y			191.164 k_Y^2 93.4520 k_Y^2 19.4484 k_Y^2 6.43052 k_Y^2 99.3632 k_Y^2 48.8147 k_Y^2 2.46429 k_Y^2 1.35745 k_Y^2 462.494 k_Y^2 0.380	188.68 k_Y^2 92.2321 k_Y^2 18.8051 k_Y^2 6.291 k_Y^2 97.7744 k_Y^2 48.0319 k_Y^2 2.35189 k_Y^2 1.31015 k_Y^2 455.476 k_Y^2 0.366
$D_3^*(2750)^-$	1^3D_3	$D^0\pi^-$ $D^-\pi^0$ $D_s^-K^0$ $D^-\eta$ $D^{*0}\pi^-$ $D^{*-}\pi^0$ $D_s^{*-}K^0$ $D^{*-}\eta$ Total k_Y			226.341 k_Y^2 110.734 k_Y^2 26.6515 k_Y^2 8.49284 k_Y^2 122.268 k_Y^2 60.1023 k_Y^2 4.34870 k_Y^2 2.10648 k_Y^2 561.045 k_Y^2 0.433	
$D_J(3000)^0$	3^1S_0	$D^{*+}\pi^-$ $D^{*0}\pi^0$ $D_s^{*+}K^-$ $D^{*0}\eta$ Total g_H^\dagger			3216.82 $g_H^{\dagger 2}$ 1623.35 $g_H^{\dagger 2}$ 1434.74 $g_H^{\dagger 2}$ 305.64 $g_H^{\dagger 2}$ 6580.55 $g_H^{\dagger 2}$ 0.169	
$D_J(3000)^0$	2^3P_1	$D^{*+}\pi^-$ $D^{*0}\pi^0$ $D_s^{*+}K^-$ $D^{*0}\eta$ Total $h_S^{\dagger 2}$			3315.44 $h_S^{\dagger 2}$ 1669.56 $h_S^{\dagger 2}$ 2409.03 $h_S^{\dagger 2}$ 515.393 $h_S^{\dagger 2}$ 7909.42 $h_S^{\dagger 2}$ 0.154	
$D_J^*(3000)^0$	3^3S_1	$D^+\pi^-$ $D^0\pi^0$ $D_s^+K^-$ $D^0\eta$ $D^{*+}\pi^-$ $D^{*0}\pi^0$ $D_s^{*+}K^-$ $D^{*0}\eta$ Total g_H^\dagger			1493.41 $g_H^{\dagger 2}$ 753.344 $g_H^{\dagger 2}$ 867.203 $g_H^{\dagger 2}$ 170.321 $g_H^{\dagger 2}$ 2338.80 $g_H^{\dagger 2}$ 1179.62 $g_H^{\dagger 2}$ 1116.37 $g_H^{\dagger 2}$ 233.034 $g_H^{\dagger 2}$ 8152.1 $g_H^{\dagger 2}$ 0.116	
$D_J^*(3000)^0$	2^3P_2	$D^+\pi^-$ $D^0\pi^0$ $D_s^+K^-$ $D^0\eta$ $D^{*+}\pi^-$ $D^{*0}\pi^0$ $D_s^{*+}K^-$ $D^{*0}\eta$ Total h_T^\dagger			2003.50 $h_T^{\dagger 2}$ 1018.38 $h_T^{\dagger 2}$ 782.29 $h_T^{\dagger 2}$ 177.739 $h_T^{\dagger 2}$ 1904.84 $h_T^{\dagger 2}$ 967.421 $h_T^{\dagger 2}$ 537.317 $h_T^{\dagger 2}$ 134.843 $h_T^{\dagger 2}$ 7526.33 $h_T^{\dagger 2}$ 0.121	

continued...

TABLE III. The strong decay widths of nonstrange charmed mesons with possible quantum state assignments (in MeV).

Meson	$\mathcal{N}^{2S+1}L_J$	Decay mode	LHCb(2016) [1]	LHCb(2015) [2]	LHCb(2013) [3]	BABAR(2010) [4]
$D_J^*(3000)^0$	1^3F_2	$D^+\pi^-$ $D^0\pi^0$ $D_s^+K^-$ $D^0\eta$ $D^{*+}\pi^-$ $D^{*0}\pi^0$ $D_s^{*+}K^-$ $D^{*0}\eta$ Total k_Z			1031.35 k_Z^2 527.383 k_Z^2 380.859 k_Z^2 101.565 k_Z^2 354.650 k_Z^2 181.010 k_Z^2 92.3905 k_Z^2 28.1319 k_Z^2 2697.34 k_Z^2	0.202
$D_J^*(3000)^0$	1^3F_4	$D^+\pi^-$ $D^0\pi^0$ $D_s^+K^-$ $D^0\eta$ $D^{*+}\pi^-$ $D^{*0}\pi^0$ $D_s^{*+}K^-$ $D^{*0}\eta$ Total k_R			2414.64 k_R^2 1246.21 k_R^2 426.29 k_R^2 129.615 k_R^2 1253.51 k_R^2 645.513 k_R^2 123.484 k_R^2 44.7903 k_R^2 6284.05 k_R^2	0.132
$D_2^*(3000)^0$	3^3P_2	$D^+\pi^-$ $D^0\pi^0$ $D_s^+K^-$ $D^0\eta$ $D^{*+}\pi^-$ $D^{*0}\pi^0$ $D_s^{*+}K^-$ $D^{*0}\eta$ Total h_T^\dagger	3844.03 $h_T^{\ddagger 2}$ 1946.41 $h_T^{\ddagger 2}$ 1977.59 $h_T^{\ddagger 2}$ 412.518 $h_T^{\ddagger 2}$ 4062.86 $h_T^{\ddagger 2}$ 2055.30 $h_T^{\ddagger 2}$ 1749.53 $h_T^{\ddagger 2}$ 386.989 $h_T^{\ddagger 2}$ 16435.2 h_T^\dagger 0.106			
$D_2^*(3000)^0$	1^3F_2	$D^+\pi^-$ $D^0\pi^0$ $D_s^+K^-$ $D^0\eta$ $D^{*+}\pi^-$ $D^{*0}\pi^0$ $D_s^{*+}K^-$ $D^{*0}\eta$ Total k_Z	2622.01 k_Z^2 1334.12 k_Z^2 1289.27 k_Z^2 306.433 k_Z^2 1043.40 k_Z^2 529.912 k_Z^2 421.817 k_Z^2 108.876 k_Z^2 7655.84 k_Z^2			0.156

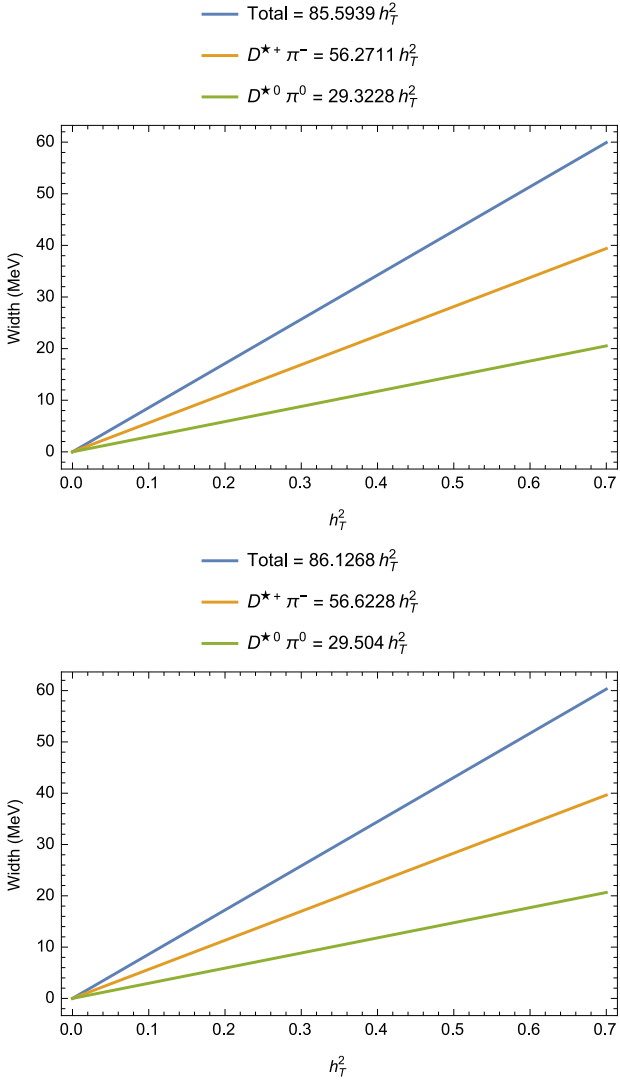


FIG. 1. Strong decay widths of $D_1(2420)^0$ (in MeV) changing with the square of the coupling h_T^2 in HQET. The masses of $D_1(2420)^0$ observed (in the decay mode $D^{*+}\pi^-$) by LHCb(2013) [3] (upper) and *BABAR*(2010) [4] (lower) are used.

$$S_a = \frac{1+\gamma}{2} [P_{1a}^\mu \gamma_\mu \gamma_5 - P_{0a}^*], \quad (2)$$

$$T_a^\mu = \frac{1+\gamma}{2} \left\{ P_{2a}^{*\mu\nu} \gamma_\nu - P_{1a\nu} \sqrt{\frac{3}{2}} \gamma_5 \left[g^{\mu\nu} - \frac{\gamma^\nu(\gamma^\mu - v^\mu)}{3} \right] \right\}, \quad (3)$$

$$X_a^\mu = \frac{1+\gamma}{2} \left\{ P_{2a}^{\mu\nu} \gamma_5 \gamma_\nu - P_{1a\nu}^* \sqrt{\frac{3}{2}} \left[g^{\mu\nu} - \frac{\gamma^\nu(\gamma^\mu + v^\mu)}{3} \right] \right\}, \quad (4)$$

$$Y_a^{\mu\nu} = \frac{1+\gamma}{2} \left\{ P_{3a}^{*\mu\nu\sigma} \gamma_\sigma - P_{2a}^{\alpha\beta} \sqrt{\frac{5}{3}} \gamma_5 \left[g_\alpha^\mu g_\beta^\nu - \frac{g_\beta^\nu \gamma_\alpha (\gamma^\mu - v^\mu)}{5} - \frac{g_\alpha^\mu \gamma_\beta (\gamma^\mu - v^\nu)}{5} \right] \right\}, \quad (5)$$

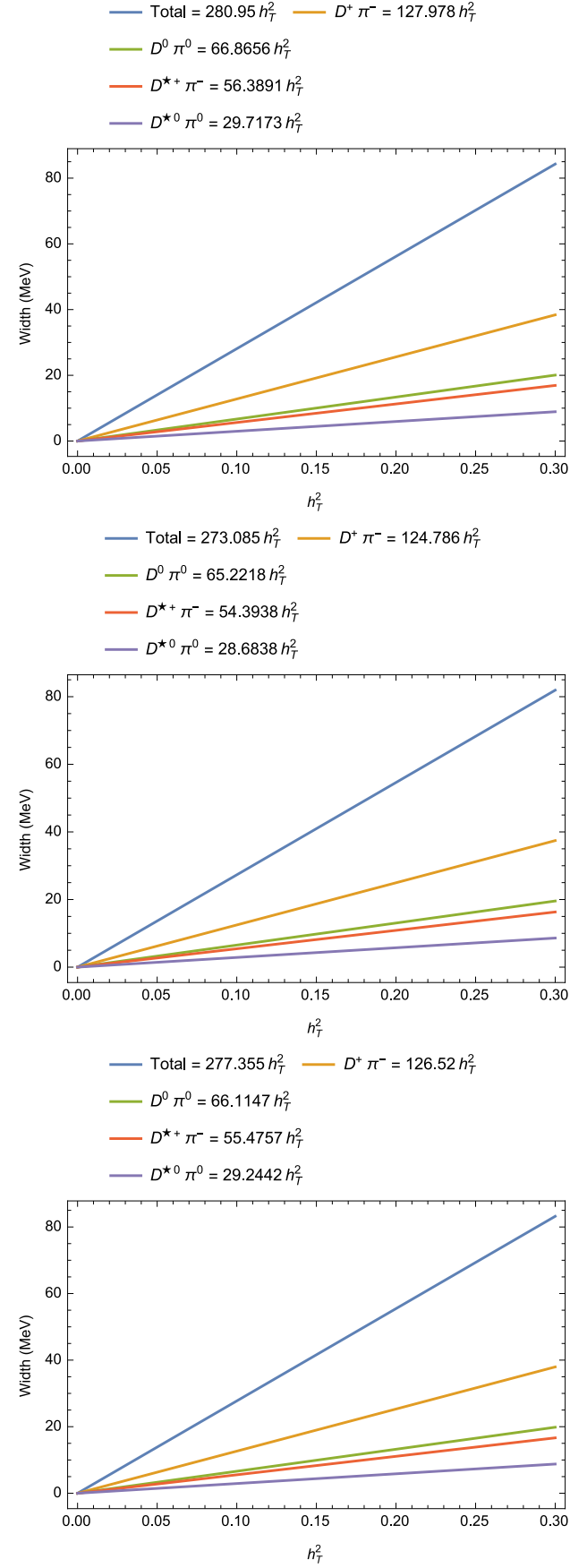
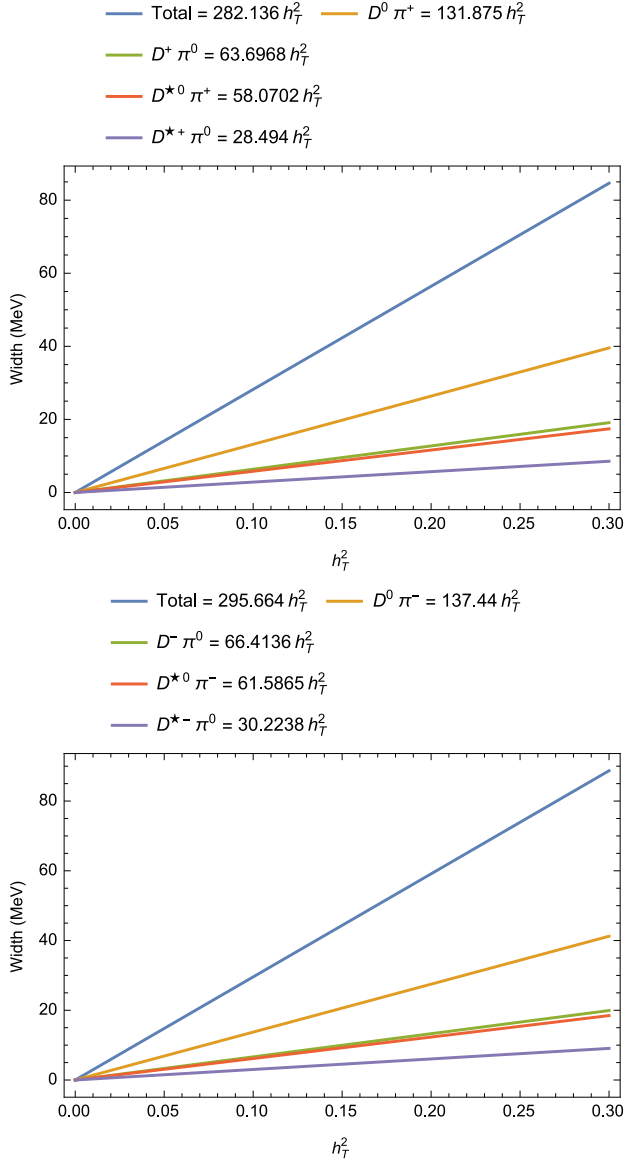
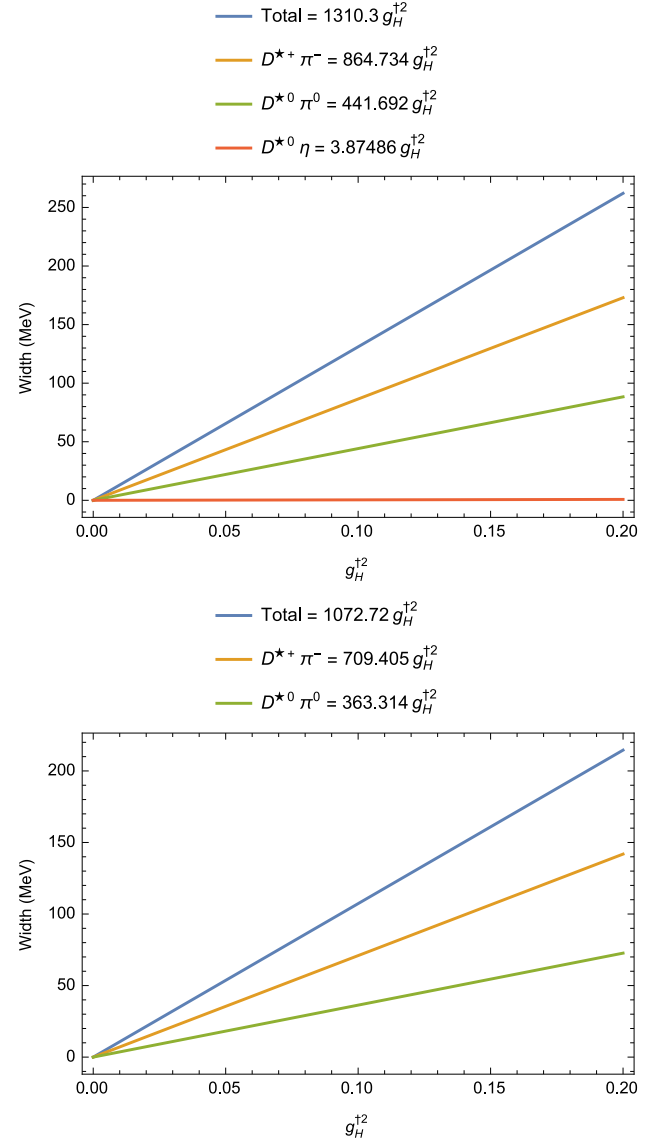


FIG. 2. Strong decay widths of $D_2^*(2460)^0$ (in MeV) changing with the square of the coupling h_T^2 in HQET. The masses of $D_2^*(2460)^0$ observed (in the decay mode $D^+ \pi^-$) by LHCb(2016) [1] (upper), LHCb(2013) [3] (middle) and *BABAR*(2010) [4] (lower) are used.



$$Z_a^{\mu\nu} = \frac{1+\gamma}{2} \left\{ P_{3a}^{\mu\nu\sigma} \gamma_5 \gamma_\sigma - P_{2a}^{*\alpha\beta} \sqrt{\frac{5}{3}} \left[g_\alpha^\mu g_\beta^\nu - \frac{g_\beta^\nu \gamma_\alpha (\gamma^\mu + v^\mu)}{5} - \frac{g_\alpha^\mu \gamma_\beta (\gamma^\nu + v^\nu)}{5} \right] \right\}, \quad (6)$$



$$R_a^{\mu\nu\rho} = \frac{1+\gamma}{2} \left\{ P_{4a}^{*\mu\nu\rho\sigma} \gamma_5 \gamma_\sigma - P_{3a}^{\alpha\beta\tau} \sqrt{\frac{7}{4}} \left[g_\alpha^\mu g_\beta^\nu g_\tau^\rho - \frac{g_\beta^\nu g_\tau^\rho \gamma_\alpha (\gamma^\mu - v^\mu)}{7} - \frac{g_\alpha^\mu g_\tau^\rho \gamma_\beta (\gamma^\nu - v^\nu)}{7} - \frac{g_\alpha^\mu g_\beta^\nu \gamma_\tau (\gamma^\rho - v^\rho)}{7} \right] \right\}. \quad (7)$$

where a ($= u, d$ or s) is the $SU(3)$ light quark flavor representation and ν gives the meson four velocity and is conserved in strong interactions. The heavy meson field operators P and P^* (see Eqs. (1) to (7)) contain a

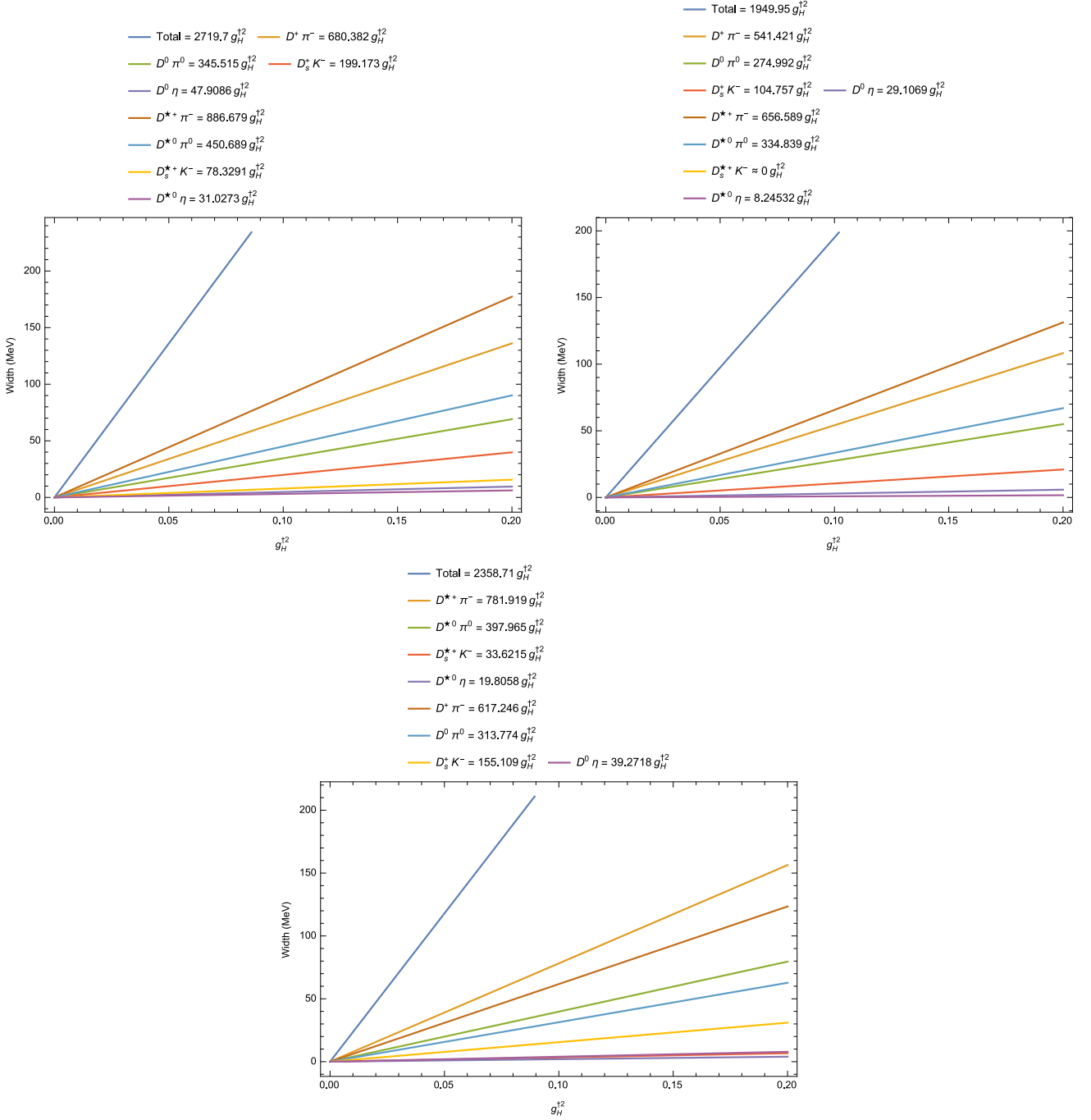


FIG. 5. Strong decay widths of $D_J^*(2600)^0$ (in MeV) changing with the square of the coupling g_H^{12} in HQET. The masses of $D_J^*(2600)^0$ observed (in the decay mode $D^+ \pi^-$) by LHCb(2016) [1] (upper left) and BABAR(2010) [4] (upper right), and (in the decay mode $D^{*+} \pi^-$) by LHCb(2013) [3] (lower) are used.

factor $\sqrt{m_Q}$ having a mass dimension $\frac{3}{2}$, which annihilate the mesons with four-velocity ν . Eq. (1) is for s wave mesons; Eq. (2) and (3) for p wave mesons; Eq. (4) and (5) for d wave mesons, and Eq. (6) and (7) for f wave mesons. The strong decays take place with the emission of light pseudoscalar octet mesons. We write the matrix \mathcal{M} of light pseudoscalar mesons described by the fields

$$\xi = e^{\frac{i\omega t}{f_\pi}} \text{ as,}$$

$$\mathcal{M} = \begin{pmatrix} \frac{1}{\sqrt{2}}\pi^0 + \frac{1}{\sqrt{6}}\eta & \pi^+ & K^+ \\ \pi^- & -\frac{1}{\sqrt{2}}\pi^0 + \frac{1}{\sqrt{6}}\eta & K^0 \\ K^- & \bar{K}^0 & -\sqrt{\frac{2}{3}}\eta \end{pmatrix} \quad (8)$$

where $f_\pi = 130.2$ MeV. Refs. [31, 36] also study the strong decays of heavy mesons along with the light vector

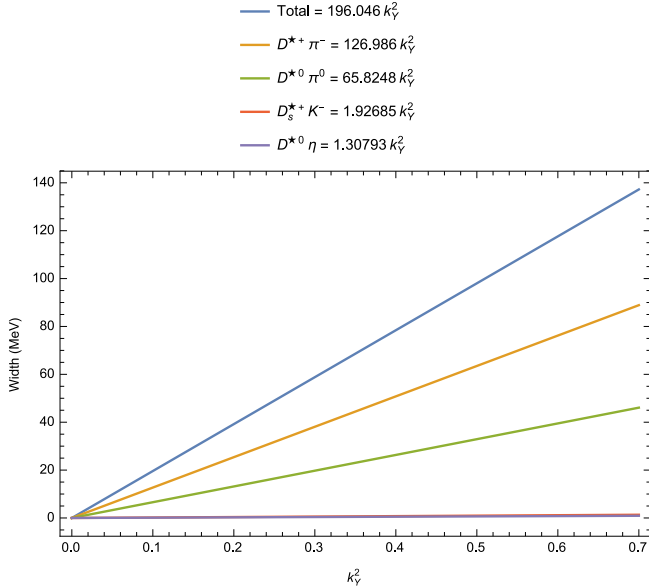


FIG. 6. Strong decay widths of $D(2740)^0$ (in MeV) changing with the square of the coupling k_Y^2 in HQET. The mass of $D(2740)^0$ observed (in the decay mode $D^{*+}\pi^-$) by LHCb(2013) [3] is used.

TABLE IV. Quantum number assignment of excited D mesons through strong decays analysis.

$N^{2S+1}L_J$	J^P	Exp. [5] (in GeV)
1^1P_1	1^+	$2.420 D_1(2420)^0$
		$2.423 D_1(2420)^{\pm}$
1^3P_2	2^+	$2.460 D_2^*(2460)^0$
		$2.465 D_2^*(2460)^{\pm}$
2^1S_0	0^-	$2.564 D(2550)^0$
2^3S_1	1^-	$2.623 D_1^*(2600)$
1^3D_2	2^-	$2.737 D(2740)^0$ [3]
1^3D_3	3^-	$2.764 D_3^*(2750)$
2^3P_1	1^+	$2.972 D_J(3000)^0$ [3]
2^3P_2	2^+	$3.008 D_J^*(3000)^0$ [3]
1^3F_2	2^+	$3.214 D_2^*(3000)^0$ [1]

mesons (ρ , ω , K and ϕ). The effective heavy meson chiral Lagrangians \mathcal{L}_H , \mathcal{L}_S , \mathcal{L}_T , \mathcal{L}_X , \mathcal{L}_Y , \mathcal{L}_Z and \mathcal{L}_R describe the two body strong interactions by an exchange of light pseudoscalar mesons, are taken from [32],

$$\mathcal{L}_H = g_H \text{Tr}[\bar{H}_a H_b \gamma_\mu \gamma_5 \mathcal{A}_{ba}^\mu], \quad (9)$$

$$\mathcal{L}_S = h_S \text{Tr}[\bar{H}_a S_b \gamma_\mu \gamma_5 \mathcal{A}_{ba}^\mu] + H.C., \quad (10)$$

$$\mathcal{L}_T = \frac{h_T}{\Lambda_\chi} \text{Tr}[\bar{H}_a T_b^\mu (iD_\mu \mathcal{A} + i\mathcal{P}\mathcal{A}^\mu)_{ba} \gamma_5] + H.C., \quad (11)$$

$$\mathcal{L}_X = \frac{k_X}{\Lambda_\chi} \text{Tr}[\bar{H}_a X_b^\mu (iD_\mu \mathcal{A} + i\mathcal{P}\mathcal{A}^\mu)_{ba} \gamma_5] + H.C., \quad (12)$$

TABLE V. Fitted parameters of the D mesons parent and daughter Regge trajectories in (J, M^2) plane with natural and unnatural parity.

	α (GeV ⁻²)	α_0	α (GeV ⁻²)	α_0
Parent	0.49366	-0.98699	0.41996	-1.46046
Daughter	0.46114	-2.17271	—	—

TABLE VI. Fitted parameters of the D mesons Regge trajectories in (n_r, M^2) plane.

Meson	β (GeV ⁻²)	β_0
D^0	0.32295	-1.12310
$D^*(2007)^0$	0.35055	-1.41181
$D_2^*(2460)^0$	0.33397	-2.02195

$$\begin{aligned} \mathcal{L}_Y = & \frac{1}{\Lambda_\chi^2} \text{Tr}[\bar{H}_a Y_b^{\mu\nu} [k_1^Y \{D_\mu, D_\nu\} \mathcal{A}_\lambda \\ & + k_2^Y (D_\mu D_\lambda \mathcal{A}_\nu + D_\nu D_\lambda \mathcal{A}_\mu)]_{ba} \gamma^\lambda \gamma_5] + H.C., \end{aligned} \quad (13)$$

$$\begin{aligned} \mathcal{L}_Z = & \frac{1}{\Lambda_\chi^2} \text{Tr}[\bar{H}_a Z_b^{\mu\nu} [k_1^Z \{D_\mu, D_\nu\} \mathcal{A}_\lambda \\ & + k_2^Z (D_\mu D_\lambda \mathcal{A}_\nu + D_\nu D_\lambda \mathcal{A}_\mu)]_{ba} \gamma^\lambda \gamma_5] + H.C., \end{aligned} \quad (14)$$

$$\begin{aligned} \mathcal{L}_R = & \frac{1}{\Lambda_\chi^3} \text{Tr}[\bar{H}_a R_b^{\mu\nu\rho} [k_1^R \{D_\mu, D_\nu, D_\rho\} \mathcal{A}_\lambda \\ & + k_2^R (\{D_\mu, D_\rho\} D_\lambda \mathcal{A}_\nu \\ & + \{D_\nu, D_\rho\} D_\lambda \mathcal{A}_\mu \{D_\mu, D_\nu\} D_\lambda \mathcal{A}_\rho)]_{ba} \gamma^\lambda \gamma_5 \\ & + H.C., \end{aligned} \quad (15)$$

TABLE VII. The masses of nonstrange charmed meson states (in GeV) lying on the 1^3S_1 , 2^3S_1 and 1^1S_0 Regge lines in (J, M^2) plane.

State	1^3S_1	1^3P_2	1^3D_3	1^3F_4
Present	2.007 [5]	2.460 [5]	2.843	3.179
Ref. [8]	2.041	2.502	2.833	3.132
Ref. [9]	2.038	2.501	2.833	3.113
Ref. [11]	2.010	2.460	2.863	3.187
Ref. [12]	2.005	2.460	2.799	3.101
State	2^3S_1	2^3P_2	2^3D_3	2^3F_4
Present	2.623 [5]	3.008 [5]	3.349	3.659
Ref. [8]	2.643	2.957	3.226	3.466
Ref. [9]	2.645	2.957	3.226	—
Ref. [11]	2.632	3.012	3.335	3.610
State	1^1S_0	1^1P_1	1^1D_2	1^1F_3
Present	1.865 [5]	2.420 [5]	2.870	3.259
Ref. [8]	1.877	2.456	2.816	3.108
Ref. [9]	1.874	2.457	2.827	3.123
Ref. [11]	1.871	2.426	2.806	3.129
Ref. [12]	1.868	2.417	2.775	3.074

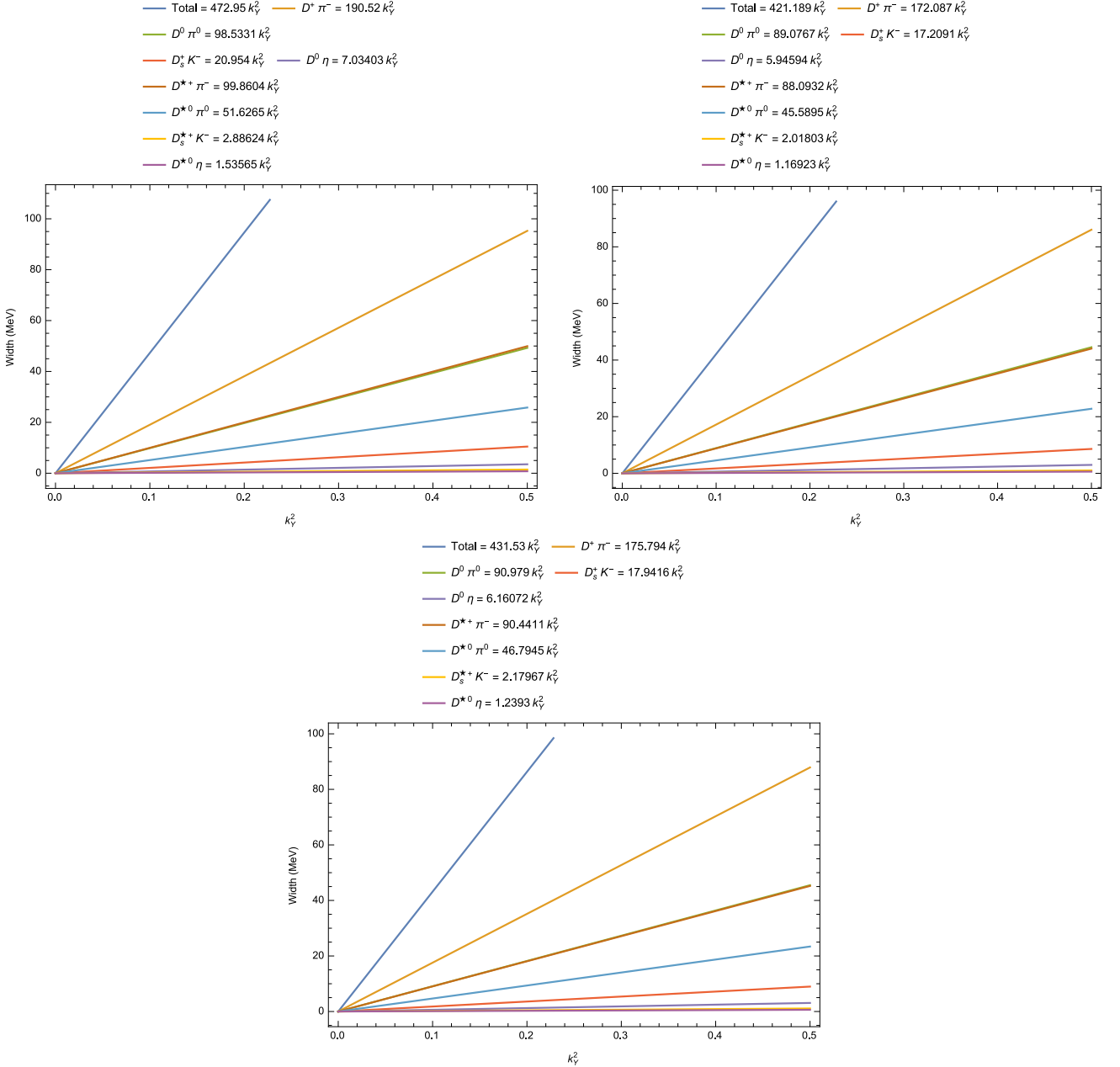


FIG. 7. Strong decay widths of $D_3^*(2750)^0$ (in MeV) changing with the square of the coupling k_Y^2 in HQET. The masses of $D_3^*(2750)^0$ observed (in the decay mode $D^+\pi^-$) by LHCb(2016) [1] (upper left), LHCb(2013) [3] (upper right) and BABAR(2010) [4] (lower) are used.

where vector and axial-vector operators are,

$$\mathcal{V}_{\mu ba} = \frac{1}{2}(\xi^\dagger \partial_\mu \xi + \xi \partial_\mu \xi^\dagger)_{ba}, \quad (16)$$

$$\mathcal{A}_{\mu ba} = \frac{i}{2}(\xi^\dagger \partial_\mu \xi - \xi \partial_\mu \xi^\dagger)_{ba}; \quad (17)$$

and the operator, $\mathcal{D}_{\mu ba} = -\delta_{ba}\partial_\mu + \mathcal{V}_{\mu ba}$. Also here, $\{\mathcal{D}_\mu, \mathcal{D}_\nu\} = \mathcal{D}_\mu \mathcal{D}_\nu + \mathcal{D}_\nu \mathcal{D}_\mu$ and $\{\mathcal{D}_\mu, \mathcal{D}_\nu, \mathcal{D}_\rho\} = \mathcal{D}_\mu \mathcal{D}_\nu \mathcal{D}_\rho + \mathcal{D}_\mu \mathcal{D}_\rho \mathcal{D}_\nu + \mathcal{D}_\nu \mathcal{D}_\mu \mathcal{D}_\rho + \mathcal{D}_\nu \mathcal{D}_\rho \mathcal{D}_\mu + \mathcal{D}_\rho \mathcal{D}_\mu \mathcal{D}_\nu + \mathcal{D}_\rho \mathcal{D}_\nu \mathcal{D}_\mu$. Λ_χ is the chiral symmetry breaking scale and is fixed to 1 GeV.

The mass parameters $\delta m_S = m_S - m_H$, $\delta m_T = m_T - m_H$, $\delta m_X = m_X - m_H$, $\delta m_Y = m_Y - m_H$, $\delta m_Z = m_Z - m_H$, and $\delta m_R = m_R - m_H$ represent the mass splittings between the higher and the lower mass doublets described by the field H_a (see Eq. (1)). The strong running coupling constants g_H , h_S , h_T , k_X , $k_Y = k_1^Y + k_2^Y$, $k_Z = k_1^Z + k_2^Z$, and $k_R = k_1^R + k_2^R$ can be fitted to the experimental data. For $n = 2$ the coupling constants are denoted by g_H^\dagger , h_S^\dagger , h_T^\dagger , k_X^\dagger , k_Y^\dagger , k_Z^\dagger , and k_R^\dagger and for $n = 3$ they are g_H^\dagger , h_S^\dagger , h_T^\dagger , k_X^\dagger , k_Y^\dagger , k_Z^\dagger , and k_R^\dagger . g_H (in Eq. (9))

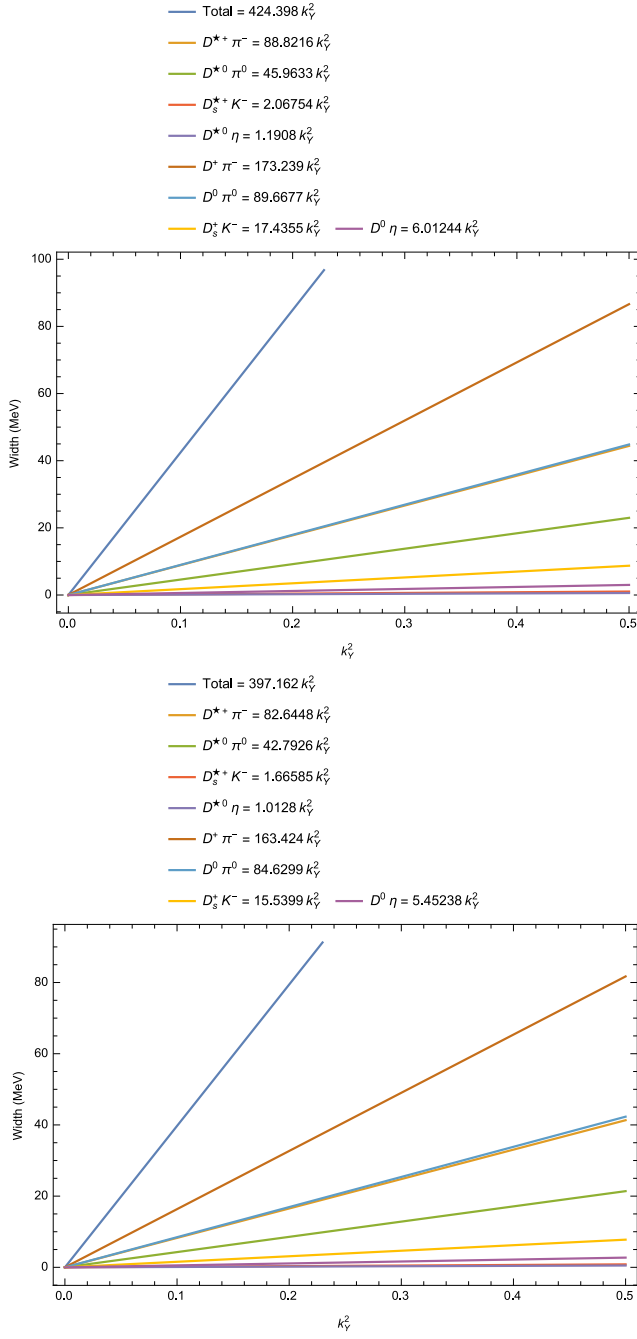


FIG. 8. Strong decay widths of $D_3^*(2750)^0$ (in MeV) changing with the square of the coupling k_Y^2 in HQET. The masses of $D_3^*(2750)^0$ observed (in the decay mode $D^{*+}\pi^-$) by LHCb(2013) [3] (upper) and BABAR(2010) [4] (lower) are used.

controls the s wave decays, h_S and h_T (in Eqs. (10) and (11)) are governs the p wave decays, k_X and k_Y (in Eqs. (12) and (13)) describe the d wave decays, and k_Z and k_R (in Eqs. (14) and (15)) are responsible for the f wave decays. Such chiral Lagrangians can determine the expressions of strong decays of heavy-light mesons into the lower mass charged and neutral $D^{(*)}$ and $D_s^{(*)}$ mesons

TABLE VIII. The masses of nonstrange charmed meson states (in GeV) lying on the 1^1S_0 , 1^3S_1 and 1^3P_2 Regge lines in (n_r, M^2) plane.

State	1^1S_0	2^1S_0	3^1S_0
Present	1.865 [5]	2.564 [5]	3.110
Ref. [8]	1.877	2.581	3.068
Ref. [9]	1.874	2.583	2.827
Ref. [11]	1.871	2.581	3.062
Ref. [12]	1.868	2.589	2.775
State	1^3S_1	2^3S_1	3^3S_1
Present	2.007 [5]	2.623 [5]	3.120
Ref. [8]	2.041	2.643	3.110
Ref. [9]	2.038	2.645	3.111
Ref. [11]	2.010	2.632	3.096
Ref. [12]	2.005	2.692	3.226
State	1^3P_2	2^3P_2	3^3P_2
Present	2.460 [5]	3.008 [5]	3.470
Ref. [8]	2.502	2.957	3.353
Ref. [9]	2.501	2.957	—
Ref. [11]	2.460	3.012	3.407
Ref. [12]	2.460	3.035	—

along with the light pseudoscalar mesons (π , η and K),

I. Decaying s wave doublet (P, P^*) or ($P^\dagger, P^{\dagger*}$) or ($P^\ddagger, P^{\ddagger*}$):

$$\Gamma(P^\dagger \rightarrow P^* \mathcal{P}) = C_{\mathcal{P}} \frac{g_H^{\dagger 2}}{2\pi f_\pi^2} \frac{P^*}{P^\dagger} |\vec{P}_{\mathcal{P}}|^3 \quad (18)$$

$$\Gamma(P^{\dagger*} \rightarrow P \mathcal{P}) = C_{\mathcal{P}} \frac{g_H^{\dagger 2}}{6\pi f_\pi^2} \frac{P}{P^{\dagger*}} |\vec{P}_{\mathcal{P}}|^3 \quad (19)$$

$$\Gamma(P^{\dagger*} \rightarrow P^* \mathcal{P}) = C_{\mathcal{P}} \frac{g_H^{\dagger 2}}{3\pi f_\pi^2} \frac{P^*}{P^{\dagger*}} |\vec{P}_{\mathcal{P}}|^3 \quad (20)$$

$$\Gamma(P^\ddagger \rightarrow P^* \mathcal{P}) = C_{\mathcal{P}} \frac{g_H^{\ddagger 2}}{2\pi f_\pi^2} \frac{P^*}{P^\ddagger} |\vec{P}_{\mathcal{P}}|^3 \quad (21)$$

$$\Gamma(P^{\ddagger*} \rightarrow P \mathcal{P}) = C_{\mathcal{P}} \frac{g_H^{\ddagger 2}}{6\pi f_\pi^2} \frac{P}{P^{\ddagger*}} |\vec{P}_{\mathcal{P}}|^3 \quad (22)$$

$$\Gamma(P^{\ddagger*} \rightarrow P^* \mathcal{P}) = C_{\mathcal{P}} \frac{g_H^{\ddagger 2}}{3\pi f_\pi^2} \frac{P^*}{P^{\ddagger*}} |\vec{P}_{\mathcal{P}}|^3 \quad (23)$$

II. Decaying p wave doublets (P_0^*, P_1') and (P_1, P_2^*) or ($P_0^{\dagger*}, P_1^{\dagger'}$) and ($P_1^\dagger, P_2^{\dagger*}$) or ($P_0^{\ddagger*}, P_1^{\ddagger'}$) and ($P_1^\ddagger, P_2^{\ddagger*}$):

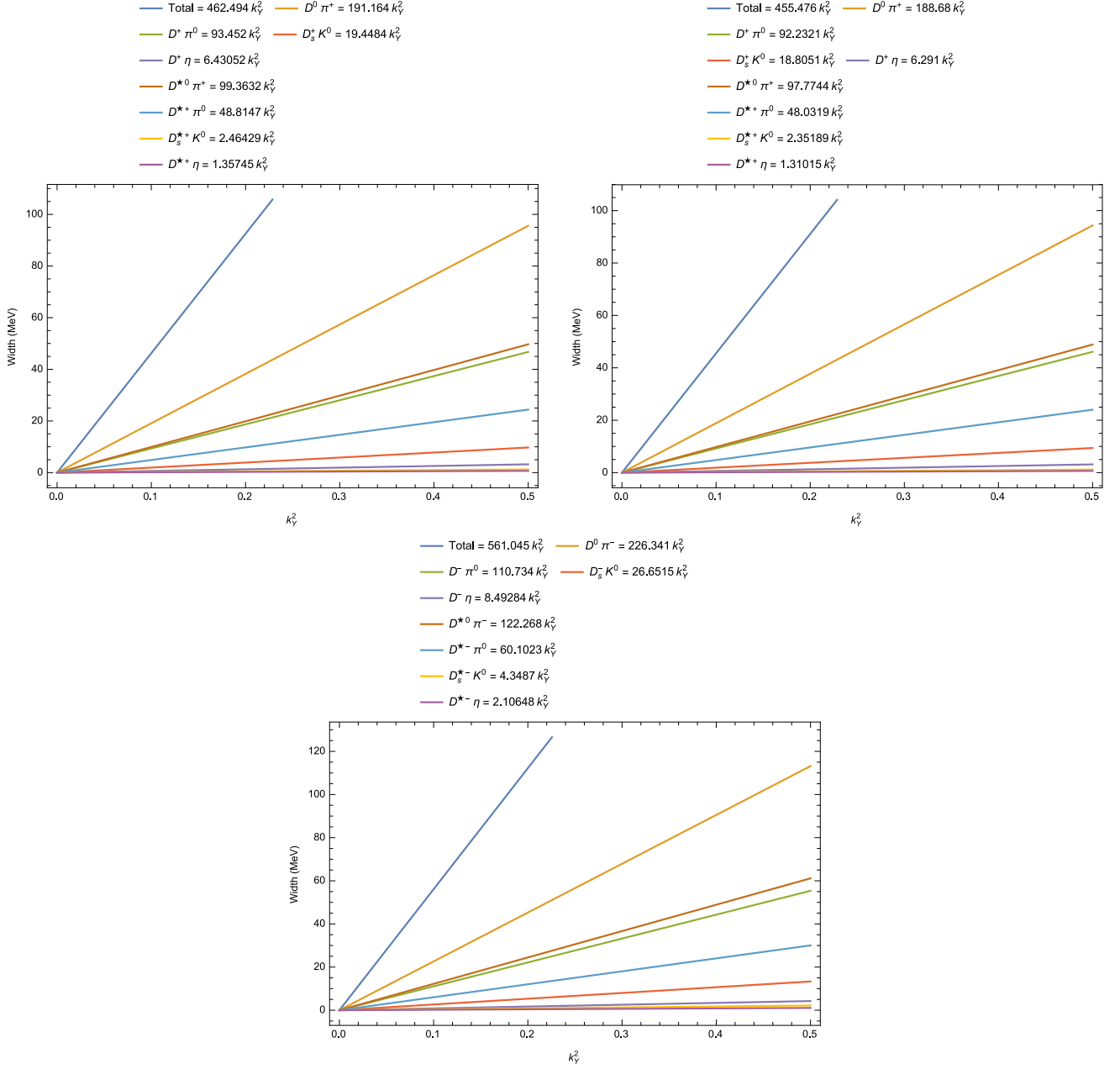


FIG. 9. Strong decay widths of $D_3^*(2750)^+$ (upper) and $D_3^*(2750)^-$ (lower) (in MeV) changing with the square of the coupling k_Y^2 in HQET. The masses of $D_3^*(2750)^+$ observed (in the decay mode $D^0\pi^+$) by LHCb(2013) [3] (upper left) and BABAR(2010) [4] (upper right), and (in the decay mode $D^0\pi^-$) by LHCb(2015) [2] (lower) are used.

$$\Gamma(P_1^{\dagger'} \rightarrow P^*\mathcal{P}) = C_{\mathcal{P}} \frac{h_S^{\dagger 2}}{2\pi f_{\pi}^2} \frac{P^*}{P_1^{\dagger'}} [m_{\mathcal{P}}^2 + |\vec{P}_{\mathcal{P}}|^2] |\vec{P}_{\mathcal{P}}| \quad (24)$$

$$\Gamma(P_1 \rightarrow P^*\mathcal{P}) = C_{\mathcal{P}} \frac{2h_T^2}{3\pi f_{\pi}^2} \frac{P^*}{P_1} |\vec{P}_{\mathcal{P}}|^5 \quad (25)$$

$$\Gamma(P_2^* \rightarrow P\mathcal{P}) = C_{\mathcal{P}} \frac{4h_T^2}{15\pi f_{\pi}^2} \frac{P}{P_2^*} |\vec{P}_{\mathcal{P}}|^5 \quad (26)$$

$$\Gamma(P_2^* \rightarrow P^*\mathcal{P}) = C_{\mathcal{P}} \frac{2h_T^2}{5\pi f_{\pi}^2} \frac{P^*}{P_2^*} |\vec{P}_{\mathcal{P}}|^5 \quad (27)$$

$$\Gamma(P_2^{\dagger *} \rightarrow P\mathcal{P}) = C_{\mathcal{P}} \frac{4h_T^{\dagger 2}}{15\pi f_{\pi}^2} \frac{P}{P_2^{\dagger *}} |\vec{P}_{\mathcal{P}}|^5 \quad (28)$$

$$\Gamma(P_2^{\dagger *} \rightarrow P^*\mathcal{P}) = C_{\mathcal{P}} \frac{2h_T^{\dagger 2}}{5\pi f_{\pi}^2} \frac{P^*}{P_2^{\dagger *}} |\vec{P}_{\mathcal{P}}|^5 \quad (29)$$

TABLE IX. Strong decay widths (in MeV), ratio and branching fraction of nonstrange charmed mesons lying on the Regge lines with possible quantum number assignments.

$\mathcal{N}^{2S+1}L_J$	Decay mode	Decay width	Ratio	Branching fraction
1^1D_2	$D^{*+}\pi^-$	$1772.11k_X^2$	1	52.3
	$D^{*0}\pi^0$	$901.224k_X^2$	0.51	26.6
	$D_s^{*+}K^-$	$553.089k_X^2$	0.31	16.32
	$D^{*0}\eta$	$160.782k_X^2$	0.09	4.74
	Total	$3388.20k_X^2$		
1^3D_3	$D^+\pi^-$	$290.925k_Y^2$	1	37.89
	$D^0\pi^0$	$149.953k_Y^2$	0.52	19.53
	$D_s^+K^-$	$45.1974k_Y^2$	0.16	5.89
	$D^0\eta$	$13.6889k_Y^2$	0.05	4.7
	$D^{*+}\pi^-$	$167.347k_Y^2$	0.58	21.79
	$D^{*0}\pi^0$	$86.1774k_Y^2$	0.3	29.62
	$D_s^{*+}K^-$	$10.3364k_Y^2$	0.04	3.55
	$D^{*0}\eta$	$4.24088k_Y^2$	0.01	1.46
	Total	$767.866k_Y^2$		
3^1S_0	$D^{*+}\pi^-$	$4389.38g_H^{\frac{1}{2}}$	1	46.14
	$D^{*0}\pi^0$	$2210.97g_H^{\frac{1}{2}}$	0.5	23.24
	$D_s^{*+}K^-$	$2427.41g_H^{\frac{1}{2}}$	0.55	25.52
	$D^{*0}\eta$	$484.987g_H^{\frac{1}{2}}$	0.11	11.05
	Total	$9512.75g_H^{\frac{1}{2}}$		
3^3S_1	$D^+\pi^-$	$1837.20g_H^{\frac{1}{2}}$	1	17.23
	$D^0\pi^0$	$925.499g_H^{\frac{1}{2}}$	0.5	8.68
	$D_s^+K^-$	$1180.56g_H^{\frac{1}{2}}$	0.64	11.07
	$D^0\eta$	$224.751g_H^{\frac{1}{2}}$	0.12	2.11
	$D^{*+}\pi^-$	$2987.19g_H^{\frac{1}{2}}$	1.62	28.01
	$D^{*0}\pi^0$	$1504.51g_H^{\frac{1}{2}}$	0.82	14.11
	$D_s^{*+}K^-$	$1671.63g_H^{\frac{1}{2}}$	0.91	15.67
	$D^{*0}\eta$	$332.810g_H^{\frac{1}{2}}$	0.18	3.12
	Total	$10664.15g_H^{\frac{1}{2}}$		
1^1F_3	$D^{*+}\pi^-$	$3211.24k_Z^2$	1	48.85
	$D^{*0}\pi^0$	$1629.54k_Z^2$	0.51	24.79
	$D_s^{*+}K^-$	$1384.61k_Z^2$	0.43	21.06
	$D^{*0}\eta$	$348.403k_Z^2$	0.11	5.3
	Total	$6573.79k_Z^2$		
1^3F_4	$D^+\pi^-$	$6784.48k_R^2$	1	34.1
	$D^0\pi^0$	$3480.78k_R^2$	0.51	17.49
	$D_s^+K^-$	$1841.32k_R^2$	0.27	9.25
	$D^0\eta$	$490.200k_R^2$	0.07	2.46
	$D^{*+}\pi^-$	$4145.64k_R^2$	0.61	20.84
	$D^{*0}\pi^0$	$2121.85k_R^2$	0.31	10.66
	$D_s^{*+}K^-$	$794.006k_R^2$	0.12	3.99
	$D^{*0}\eta$	$236.237k_R^2$	0.03	1.19
	Total	$19896.51k_R^2$		

continued...

$$\Gamma(P_2^{\frac{1}{2}*} \rightarrow P\mathcal{P}) = C_{\mathcal{P}} \frac{4h_T^{\frac{1}{2}}}{15\pi f_{\pi}^2} \frac{P}{P_2^{\frac{1}{2}*}} |\vec{P}_{\mathcal{P}}|^5 \quad (30)$$

$$\Gamma(P_2^{\frac{1}{2}*} \rightarrow P^*\mathcal{P}) = C_{\mathcal{P}} \frac{2h_T^{\frac{1}{2}}}{5\pi f_{\pi}^2} \frac{P^*}{P_2^{\frac{1}{2}*}} |\vec{P}_{\mathcal{P}}|^5 \quad (31)$$

III. Decaying d wave doublets (P_1^* , P_2) and (P_2' , P_3^*):

$$\Gamma(P_2 \rightarrow P^*\mathcal{P}) = C_{\mathcal{P}} \frac{2k_X^2}{3\pi f_{\pi}^2} \frac{P^*}{P_2} [m_{\mathcal{P}}^2 + |\vec{P}_{\mathcal{P}}|^2] |\vec{P}_{\mathcal{P}}|^3 \quad (32)$$

TABLE IX. Strong decay widths (in MeV), ratio and branching fraction of nonstrange charmed mesons lying on the Regge lines with possible quantum number assignments.

$\mathcal{N}^{2S+1}L_J$	Decay mode	Decay width	Ratio	Branching fraction
2^3D_3	$D^+\pi^-$	$3130.22k_Y^{\dagger 2}$	1	26.65
	$D^0\pi^0$	$1590.47k_Y^{\dagger 2}$	0.51	13.54
	$D_s^+K^-$	$1436.88k_Y^{\dagger 2}$	0.46	12.23
	$D^0\eta$	$315.141k_Y^{\dagger 2}$	0.1	2.68
	$D^{*+}\pi^-$	$2668.36k_Y^{\dagger 2}$	0.85	22.72
	$D^{*0}\pi^0$	$1353.63k_Y^{\dagger 2}$	0.43	11.52
	$D_s^{*+}K^-$	$1012.98k_Y^{\dagger 2}$	0.32	8.62
	$D^{*0}\eta$	$238.644k_Y^{\dagger 2}$	0.08	2.03
	Total	$11746.32k_Y^{\dagger 2}$		
3^3P_2	$D^+\pi^-$	$7478.9h_T^{\dagger 2}$	1	20.93
	$D^0\pi^0$	$3774.68h_T^{\dagger 2}$	0.5	10.56
	$D_s^+K^-$	$4684.67h_T^{\dagger 2}$	0.63	13.11
	$D^0\eta$	$916.581h_T^{\dagger 2}$	0.12	2.69
	$D^{*+}\pi^-$	$8640.15h_T^{\dagger 2}$	1.16	24.18
	$D^{*0}\pi^0$	$4357.18h_T^{\dagger 2}$	0.58	12.19
	$D_s^{*+}K^-$	$4886.89h_T^{\dagger 2}$	0.65	13.68
	$D^{*0}\eta$	$993.325h_T^{\dagger 2}$	0.13	2.78
	Total	$35732.4h_T^{\dagger 2}$		
2^3F_4	$D^+\pi^-$	$64151k_R^{\dagger 2}$	1	26.75
	$D^0\pi^0$	$32588k_R^{\dagger 2}$	0.51	13.59
	$D_s^+K^-$	$31378.1k_R^{\dagger 2}$	0.49	13.08
	$D^0\eta$	$6879.94k_R^{\dagger 2}$	0.11	2.87
	$D^{*+}\pi^-$	$51500.9k_R^{\dagger 2}$	0.8	21.48
	$D^{*0}\pi^0$	$26110.5k_R^{\dagger 2}$	0.41	10.89
	$D_s^{*+}K^-$	$22101.5k_R^{\dagger 2}$	0.34	9.21
	$D^{*0}\eta$	$5103.52k_R^{\dagger 2}$	0.08	2.13
	Total	$239813k_R^{\dagger 2}$		

$$\Gamma(P'_2 \rightarrow P^*\mathcal{P}) = C_{\mathcal{P}} \frac{4k_Y^2}{15\pi f_{\pi}^2} \frac{P^*}{P'_2} |\vec{P}_{\mathcal{P}}|^7 \quad (33)$$

$$\Gamma(P'^*_2 \rightarrow P^*\mathcal{P}) = C_{\mathcal{P}} \frac{8k_Z^2}{75\pi f_{\pi}^2} \frac{P^*}{P'^*_2} [m_{\mathcal{P}}^2 + |\vec{P}_{\mathcal{P}}|^2] |\vec{P}_{\mathcal{P}}|^5 \quad (39)$$

$$\Gamma(P_3^* \rightarrow P\mathcal{P}) = C_{\mathcal{P}} \frac{4k_Y^2}{35\pi f_{\pi}^2} \frac{P}{P_3^*} |\vec{P}_{\mathcal{P}}|^7 \quad (34)$$

$$\Gamma(P_3 \rightarrow P^*\mathcal{P}) = C_{\mathcal{P}} \frac{4k_Z^2}{15\pi f_{\pi}^2} \frac{P^*}{P_3} [m_{\mathcal{P}}^2 + |\vec{P}_{\mathcal{P}}|^2] |\vec{P}_{\mathcal{P}}|^5 \quad (40)$$

$$\Gamma(P_3^* \rightarrow P^*\mathcal{P}) = C_{\mathcal{P}} \frac{16k_Y^2}{105\pi f_{\pi}^2} \frac{P^*}{P_3^*} |\vec{P}_{\mathcal{P}}|^7 \quad (35)$$

$$\Gamma(P_4^* \rightarrow P\mathcal{P}) = C_{\mathcal{P}} \frac{16k_R^2}{35\pi f_{\pi}^2} \frac{P}{P_4^*} |\vec{P}_{\mathcal{P}}|^9 \quad (41)$$

$$\Gamma(P_3^{\dagger*} \rightarrow P\mathcal{P}) = C_{\mathcal{P}} \frac{4k_Y^{\dagger 2}}{35\pi f_{\pi}^2} \frac{P}{P_3^{\dagger*}} |\vec{P}_{\mathcal{P}}|^7 \quad (36)$$

$$\Gamma(P_4^* \rightarrow P^*\mathcal{P}) = C_{\mathcal{P}} \frac{4k_R^2}{7\pi f_{\pi}^2} \frac{P^*}{P_4^*} |\vec{P}_{\mathcal{P}}|^9. \quad (42)$$

$$\Gamma(P_3^{\dagger*} \rightarrow P^*\mathcal{P}) = C_{\mathcal{P}} \frac{16k_Y^{\dagger 2}}{105\pi f_{\pi}^2} \frac{P^*}{P_3^{\dagger*}} |\vec{P}_{\mathcal{P}}|^7 \quad (37)$$

$$\Gamma(P_4^{\dagger*} \rightarrow P\mathcal{P}) = C_{\mathcal{P}} \frac{16k_R^{\dagger 2}}{35\pi f_{\pi}^2} \frac{P}{P_4^{\dagger*}} |\vec{P}_{\mathcal{P}}|^9 \quad (43)$$

IV. Decaying f wave doublets (P'^*_2, P_3) and (P'_3, P_4^*):

$$\Gamma(P'^*_2 \rightarrow P\mathcal{P}) = C_{\mathcal{P}} \frac{4k_Z^2}{25\pi f_{\pi}^2} \frac{P}{P'^*_2} [m_{\mathcal{P}}^2 + |\vec{P}_{\mathcal{P}}|^2] |\vec{P}_{\mathcal{P}}|^5 \quad (38)$$

$$\Gamma(P'^*_4 \rightarrow P^*\mathcal{P}) = C_{\mathcal{P}} \frac{4k_R^{\dagger 2}}{7\pi f_{\pi}^2} \frac{P^*}{P'^*_4} |\vec{P}_{\mathcal{P}}|^9. \quad (44)$$

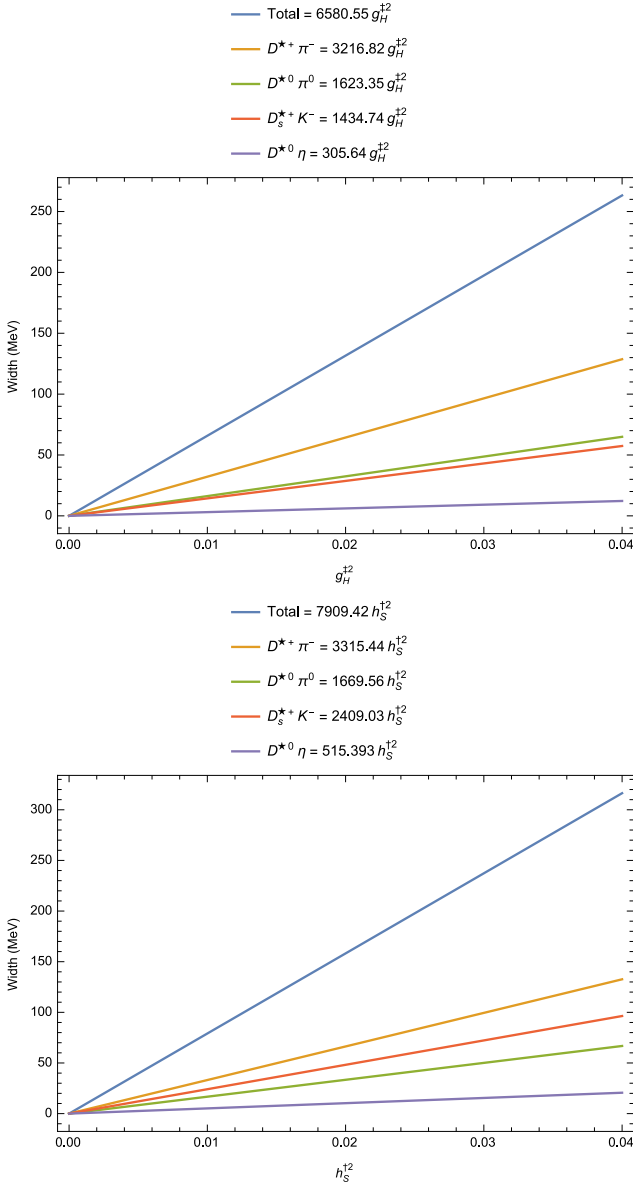


FIG. 10. Strong decay widths of $D_J(3000)^0$ as 3^1S_0 (upper) and 2^3P_1 (lower) changing with the square of the couplings $g_H^{†2}$ and $h_S^{†2}$ respectively in HQET. The mass of $D_J(3000)^0$ observed (in the decay mode $D^{*+}\pi^-$) by LHCb(2013) [3] is used.

For the decay mode $P_a \rightarrow P_b + \mathcal{P}$ we have $|\vec{P}_{\mathcal{P}}| = \sqrt{\frac{m_{P_a}^2 + m_{P_b}^2 + m_{\mathcal{P}}^2 - 2m_{P_a}m_{P_b} - 2m_{P_a}m_{\mathcal{P}} - 2m_{P_b}m_{\mathcal{P}}}{2m_{P_a}}}$; where m_{P_a} , m_{P_b} and $m_{\mathcal{P}}$ are their respective masses. The coefficients \mathcal{P} of the light pseudoscalar mesons are: $C_{\pi^\pm}, C_{K^\pm} = 1$, $C_{\pi^0} = \frac{1}{2}$ and $C_\eta = \frac{1}{6}$. The masses of the light pseudoscalar mesons and the ground state charmed mesons are taken from PDG-2018 [5]: $M_{\pi^\pm} = 139.57061$ MeV, $M_{\pi^0} = 134.9770$ MeV, $M_{K^\pm} = 493.677$ MeV, $M_{K^0} = 497.611$ MeV, $M_\eta = 547.862$ MeV, $M_{D^\pm} = 1869.65$, $M_{D^0} = 1864.84$ MeV, $M_{D^{*\pm}} = 2010.26$ MeV, $M_{D_s^{*0}} = 2006.85$ MeV, $M_{D_s^\pm} = 1969.0$ MeV, $M_{D_s^{*\pm}} = 2112.2$

MeV. In the heavy quark mass limit, the spin and flavor violations of order $\frac{1}{m_Q}$ are not taken into the consideration in this present study to avoid introducing new unknown coupling constants. The strong decay widths can provide some useful informations and are used for the classification of various mesonic states according to their total spin and parity. Also the ratio and the branching fractions among the decay widths, independent of the coupling constants, can help to identify the heavy mesons.

III. RESULTS AND DISCUSSION

Using the Eqs. (18) to (44), the strong decay rates of nonstrange singly charmed mesons ($D_2^*(2460)$, $D(2550)^0$, $D_J^*(2600)^0$, $D(2740)^0$, $D_3^*(2750)^0$, $D_J(3000)^0$, $D_J^*(3000)^0$ and $D_2^*(3000)^0$ observed by the experimental Collaborations LHCb [1–3] and *BABAR* [4]) are computed. That are presented in Table III in terms of the square of the coupling constants h_T , g_H^\dagger , k_Y , g_H^\ddagger , h_S^\dagger , h_T^\dagger , k_R and k_Z . Such a wide range of couplings are not yet observed experimentally. The present experimental facility LHCb and an upcoming project *PaNDA* [33, 34] will fit these strong couplings in near future. Theoretically, the Refs. [35–39] have studied the strong coupling constants of *s* and *p* wave ground state heavy mesons. Comparing the calculated total decay widths shown in Table III (also Figures (1) to (12) represents the strong decay rates that are changing with respect to the square of the couplings) with their respective experimentally observed decay widths listed in Table I, we determine the strong coupling constants which are presented in Table III.

The branching ratios avoid the unknown hadronic couplings and are compared with experimental observations where available. The branching ratio,

$$BR_{D_2^*(2460)^0} = \frac{\Gamma(D_2^*(2460)^0 \rightarrow D^+\pi^-)}{\Gamma(D_2^*(2460)^0 \rightarrow D^{*+}\pi^-)} \approx 2.3,$$

calculated from Ref. [1], [3] and [4]. It is in good agreement with the measurements of CLEO Collaboration 2.3 ± 0.8 [40], underestimated to ZEUS 2.8 ± 0.8 [41] and overestimated to *BABAR* 1.47 ± 0.03 [4] and ZEUS 1.4 ± 0.3 [42]. The ratio,

$$R_{D_2^*(2460)^0} = \frac{\Gamma(D_2^*(2460)^0 \rightarrow D^+\pi^-)}{\Gamma(D_2^*(2460)^0 \rightarrow D^{*+}\pi^-) + \Gamma(D_2^*(2460)^0 \rightarrow D^{*0}\pi^0)} \approx 0.70$$

from Refs. [1, 3, 4] and is close to $0.62 \pm 0.03 \pm 0.02$ of *BABAR* measurement [43]. The branching ratio,

$$BR_{D_2^*(2460)^+} = \frac{\Gamma(D_2^*(2460)^+ \rightarrow D^0\pi^+)}{\Gamma(D_2^*(2460)^+ \rightarrow D^{*0}\pi^+)} \approx 2.3$$

from [3], which is nearer to $1.9 \pm 1.1 \pm 0.3$ of CLEO measurement [44] and overestimated to ZEUS 1.1 ± 0.4 [42]. And, also the ratio

$$R_{D_2^*(2460)^+} = \frac{\Gamma(D_2^*(2460)^+ \rightarrow D^0\pi^+)}{\Gamma(D_2^*(2460)^+ \rightarrow D^{*0}\pi^+) + \Gamma(D_2^*(2460)^+ \rightarrow D^{*+}\pi^0)} \approx 0.70$$

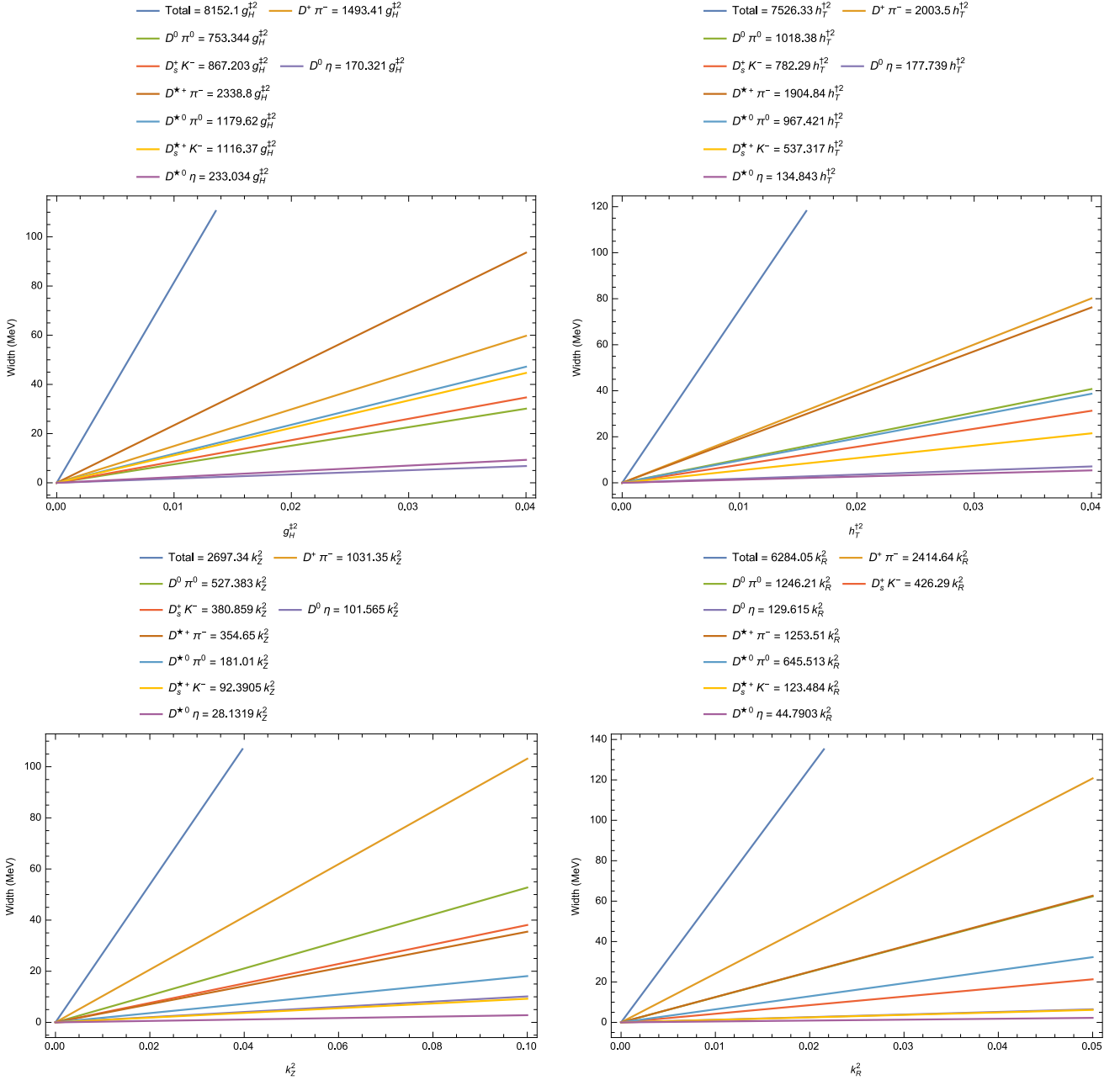


FIG. 11. Strong decay widths of $D_J^*(3000)^0$ as 3^3S_1 (upper left), 2^3P_2 (upper right), 1^3F_2 (lower left) and 1^3F_4 (lower right) changing with the square of the couplings $g_H^{\dagger 2}$, $h_T^{\dagger 2}$, k_Z^2 and k_R^2 respectively. The mass of $D_J^*(3000)^0$ observed (in the decay mode $D^+\pi^-$) by LHCb(2013) [3] is used.

≈ 0.7 from [3] close to Ref. [43]. The branching ratios,

$$BR_{D_J^*(2600)^0} = \frac{\Gamma(D_J^*(2600)^0 \rightarrow D^+\pi^-)}{\Gamma(D_J^*(2600)^0 \rightarrow D^{*+}\pi^-)} \approx 0.8$$

$$BR_{D_J^*(2750)^0} = \frac{\Gamma(D_J^*(2750)^0 \rightarrow D^+\pi^-)}{\Gamma(D_J^*(2750)^0 \rightarrow D^{*+}\pi^-)} \approx 1.9$$

calculated from Ref. [1], [3] and [4], which are overestimated to the *BABAR* measurements $BR_{D_J^*(2600)^0} = 0.32 \pm 0.02 \pm 0.09$ and $BR_{D_J^*(2750)^0} = 0.42 \pm 0.05 \pm 0.11$ [4].

Therefore, the charmed mesons $D_2^*(2460)$ and $D_J^*(2750)$ belonging to 1^3P_2 and 1^3D_3 are dominant in $D\pi$ decay mode and, $D_J^*(2600)$ with 2^3S_1 dominant in $D^*\pi$ decay. That are in accessible with the experimental observations. Moreover, the $D_1(2420)$, $D(2550)$ and $D(2740)$ are found to be spin partners of $D_2^*(2460)$, $D_J^*(2600)$ and $D_J^*(2750)$ respectively. So we write,

$$(D_1(2420), D_2^*(2460)) = (1^+, 2^+)_{\frac{3}{2}+} = (1^1P_1, 1^3P_2), \quad (45)$$

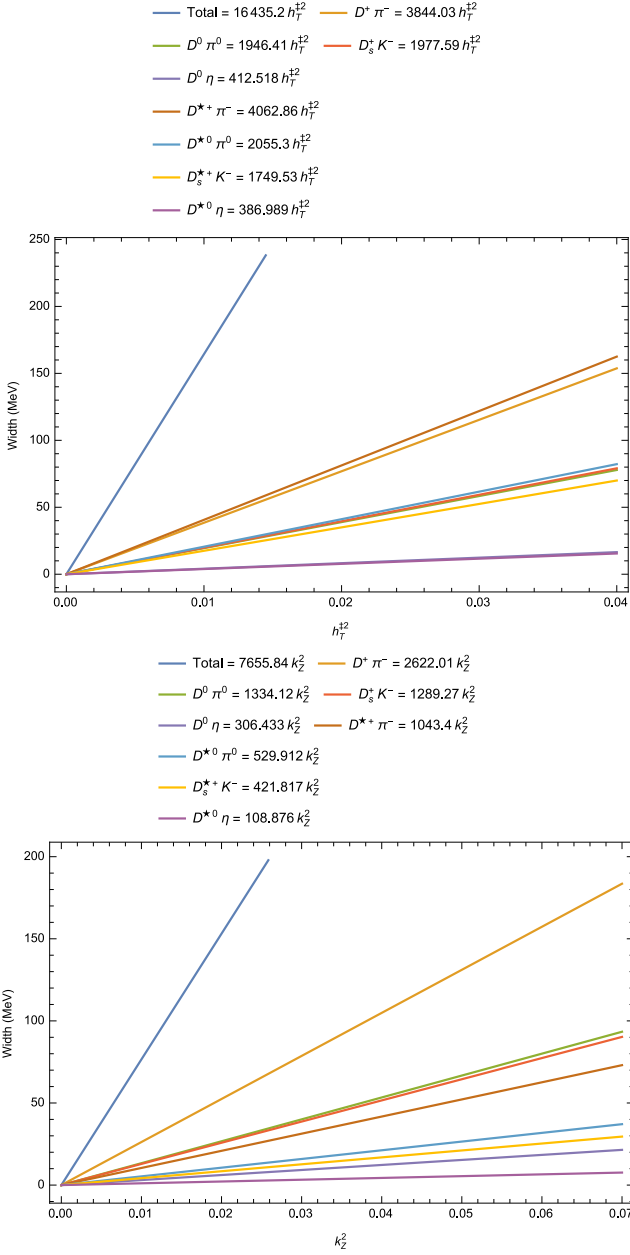


FIG. 12. Strong decay widths of $D_s^*(3000)^0$ as 3^3P_2 (upper) and 1^3F_2 (lower) changing with the square of the couplings $h_T^{±2}$ and k_Z^2 respectively. The mass of $D_s^*(3000)^0$ observed (in the decay mode $D^+\pi^-$) by LHCb(2016) [1] is used.

$$(D(2550), D_J^*(2600)) = (0^-, 1^-)_{\frac{1}{2}-} = (2^1S_0, 2^3S_1), \quad (46)$$

$$(D(2740), D_J^*(2750)) = (2^-, 3^-)_{\frac{5}{2}-} = (1^3D_2, 1^3D_3). \quad (47)$$

The mass difference $M_{D_J^*(3000)^0} - M_{D_J(3000)^0} \approx 36$ MeV. They might be from the same wave family. Experimentally, $D_J(3000)$ is measured with unnatural parity and $D_J^*(3000)$ with natural parity. So they can have an isodoublet state either $(0^-, 1^-)_{\frac{1}{2}-}$ or $(1^+, 2^+)_{\frac{3}{2}+}$. The

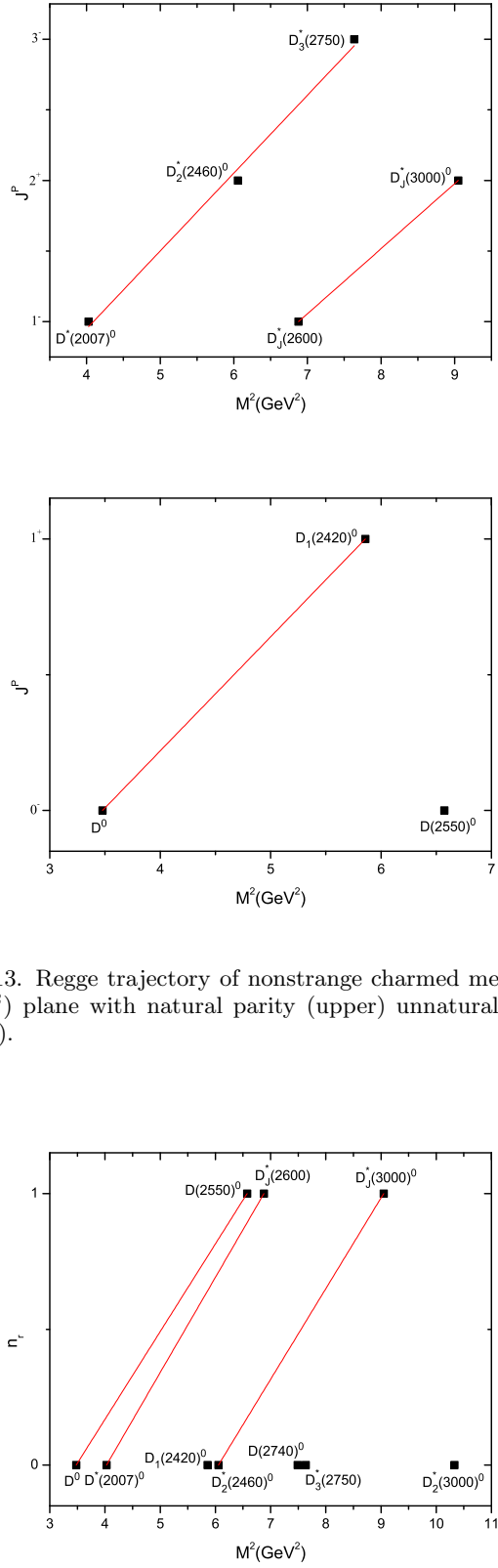


FIG. 13. Regge trajectory of nonstrange charmed mesons in (J, M^2) plane with natural parity (upper) unnatural parity (lower).

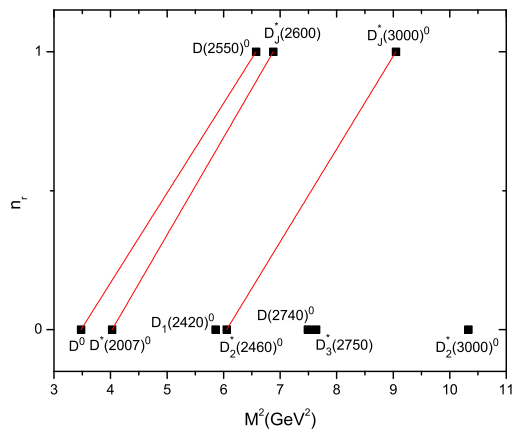


FIG. 14. Regge trajectory of nonstrange charmed mesons in (n_r, M^2) plane.

$(D_J(3000), D_J^*(3000))$ is not of an isodoublet $(1^+, 0^+)_{\frac{1}{2}+}$ because the $J^P = 0^+$ of $D_J^*(3000)$ is not possible to be heavier than $J^P = 1^+$ of $D_J(3000)$. The $D_J^*(3000)^0$ as 3^3S_1 has

$$BR_{D_J^*(3000)^0} = \frac{\Gamma(D_J^*(3000)^0 \rightarrow D^+\pi^-)}{\Gamma(D_J^*(3000)^0 \rightarrow D^+\pi^-)} \approx 0.64,$$

that means, the decay mode $D^{*+}\pi^-$ is dominant over $D^+\pi^-$. The $D_J^*(3000)^0$ as 2^3P_2 has $BR_{D_J^*(3000)^0} \geq 1$, which is in agreement with the experimental measurement. Hence,

$$(D_J(3000), D_J^*(3000)) = (1^+, 2^+)_{\frac{3}{2}+} = (2^3P_1, 2^3P_2). \quad (48)$$

The mass difference between $D_2^*(3000)^0$ and $D_J^*(3000)^0$ is approximately 206 MeV. Such a large mass difference indicate $D_2^*(3000)^0$ state is not of $2P$ state. Experimentally, its observed spin-parity is 2^+ . So it can be a candidate of 3^3P_2 or 1^3F_2 . For $D_2^*(3000)^0$ as 3^3P_2 ,

$$BR_{D_2^*(3000)^0} = \frac{\Gamma(D_2^*(3000)^0 \rightarrow D^+\pi^-)}{\Gamma(D_2^*(3000)^0 \rightarrow D^+\pi^-)} \approx 0.95,$$

i.e. the decay $D^{*+}\pi^-$ is more dominant than $D^+\pi^-$. For 1^3F_2 state, the $BR_{D_2^*(3000)^0}$ is 2.51, which is most favorable to decay in $D^+\pi^-$ and, it is in accordance with the experimental measurement. So,

$$D_2^*(3000)^0 = (2^+)_{\frac{5}{2}+} = (1^3F_2). \quad (49)$$

IV. REGGE TRAJECTORY

Spin and parity assignments of excited D mesons from the strong decays analysis are presented in Table IV with their respective PDG-2018 [5] world average masses. Using these we construct the Regge trajectory in which the total spin (or principal quantum number (n)) and the mass of hadrons are related. This can help in predicting the possible quantum states of hadrons. An investigation of meson spectrum in the non-perturbative regime of quark-gluon interactions has a great importance for understanding the dynamics of strong interactions (for details see Refs. [45, 46]). We are using the following definitions:

I. the Regge trajectory in (J, M^2) plane,

$$J = \alpha M^2 + \alpha_0; \quad (50)$$

II. and the Regge trajectory in (n_r, M^2) plane,

$$n_r = \beta M^2 + \beta_0; \quad (51)$$

where α, β are slopes, α_0, β_0 are intercepts and $n_r (= n - 1) = 0, 1, 2, \dots$ is the radial principal quantum number. The Regge trajectory in (J, M^2) plane are available with the evenness and oddness of the total spin J are respectively distinguished according to their parity $P = (-1)^J$ called natural parity and $P = (-1)^{J-1}$ called unnatural parity. Figures 13 and 14 shows the plots of Regge trajectories in (J, M^2) and (n_r, M^2) planes which are usually called Chew-Frautschi plots. The D meson states are fitted on the Regge line with sufficiently good accuracy. The parameters like Regge slopes and the intercepts are extracted from the Regge trajectories (see in Table V and VI), that estimate the masses of the states lying on these Regge trajectories. The Regge slope is assumed to be same for all D meson multiplets lying on the single Regge line.

The masses of $1^1D_2, 1^3D_3, 3^1S_0, 3^3S_1, 1^1F_3, 1^3F_4, 2^3D_3, 3^3P_2$ and 2^3F_4 states are estimated (see in Table VII and VIII). The 2.843 GeV of 1^3D_3 is overestimated to $D_3^*(2750)^0$ by a mass difference of 79 MeV. Also, the helicity distribution disfavors the identification of $D_3^*(2750)$ as a 1^3D_3 [47]. But we tentatively identify $(D_3^*(2750)^0)$ as $(3^-)_{\frac{5}{2}-}$ with $n = 1$. For $1^3D_3, 1^3F_4, 2^3D_3, 2^3F_4$ and 3^3S_1 , our results are in agreement with D. Ebert *et al.* [11] and are overestimates to the predictions of Refs. [8, 9, 12]. Such heavier masses agree with the argument that slopes of Regge trajectories decrease with quark mass increase [48–51]. The partial strong decay rates of these predicted states are calculated and presented in Table IX. These are also shown in Figures 15 to 23, where the strong decay rates change with respect to the square of the couplings. The decay mode $D^{*+}\pi^-$ is dominant in the states $1^1D_2, 3^1S_0, 3^3S_1, 1^1F_3$ and 3^3P_2 with branching fractions 52.30%, 46.14%, 28.01%, 48.85% and 24.18% respectively. And, for the $1^3D_3, 1^3F_4, 2^3D_3$ and 2^3F_4 states the $D^+\pi^-$ decay is dominant with branching fractions 37.87%, 34.09%, 26.64% and 26.74% respectively.

V. CONCLUSIONS

In this paper, we have examined the nonstrange charmed mesons $D_1(2420)^0, D_2^*(2460), D(2550)^0, D_J^*(2600)^0, D(2740)^0, D_3^*(2750), D_J(3000)^0, D_J^*(3000)^0$ and $D_2^*(3000)^0$ observed by the LHCb [1–3] and *BABAR* [4] Collaborations according to their spin, parity and masses. Their strong decays into ground state charmed mesons along with the emission of light pseudoscalar mesons (π, η, K) are analyzed in the HQET. The branching ratios among the strong decays tentatively identify the quantum numbers of nonstrange charmed mesons. The strong decay widths are retained with the square of the coupling constants $h_T, g_H^\dagger, k_Y, g_H^\dagger, h_S^\dagger, h_T^\dagger, k_R$ and k_Z , which are determined comparing those with the widths observed by experimental groups given in Table III. We identify the states $D(2550)^0, D_J^*(2600)^0, D(2740)^0$ and $D_3^*(2750)$ with spin-parity $0^-, 1^-, 2^-$

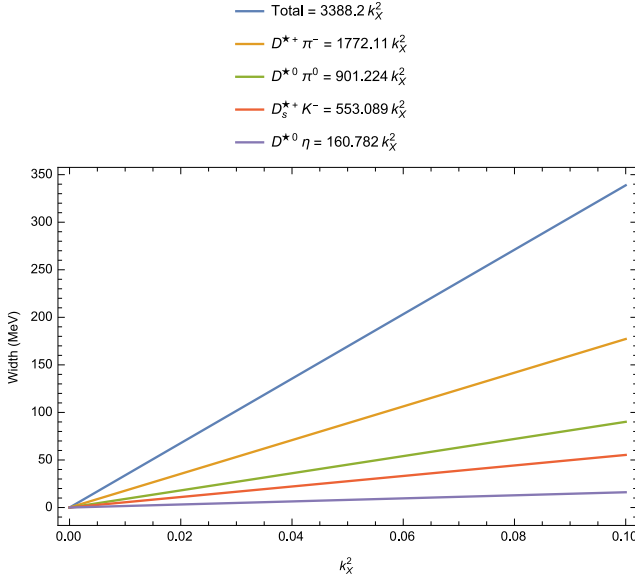


FIG. 15. Strong decay widths of 1^1D_2 (in MeV) nonstrange charmed meson state (lying on the Regge line 1^1S_0 in (n_r, M^2) plane) changing with the square of the coupling k_x^2 in HQET.

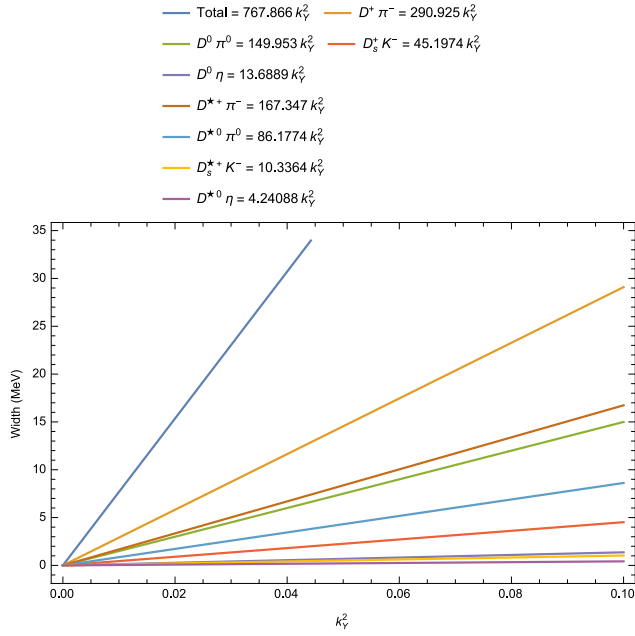


FIG. 16. Strong decay widths of 1^3D_3 (in MeV) nonstrange charmed meson state (lying on the Regge line 1^3S_1 in (J, M^2) plane) changing with the square of the coupling k_y^2 in HQET.

and 3^- respectively. They are in agreement with the strong decays analysis done by Refs. [22–26]. An unclear resonance structures near 3 GeV region motivated our present study. We tentatively assign the quantum states of $D_J(3000)^0$, $D_J^*(3000)^0$ and $D_2^*(3000)^0$ as 2^3P_1 , 2^3P_2 and 1^3F_2 respectively. The states $D_J(3000)^0$ and $D_J^*(3000)^0$ are in accordance with the predictions of

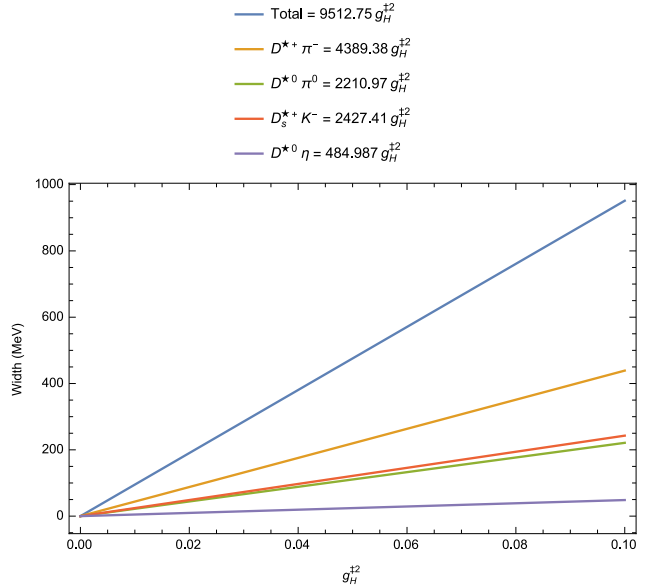


FIG. 17. Strong decay widths of 3^1S_0 (in MeV) nonstrange charmed meson state (lying on the Regge line 1^1S_0 in (n_r, M^2) plane) changing with the square of the coupling $g_H^{‡2}$ in HQET.

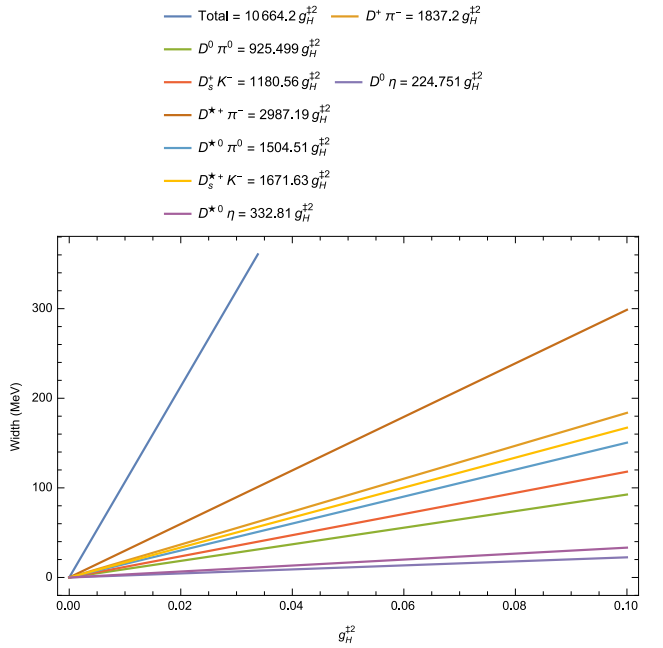


FIG. 18. Strong decay widths of 3^3S_1 (in MeV) nonstrange charmed meson state (lying on the Regge line 1^3S_1 in (n_r, M^2) plane) changing with the square of the coupling $g_H^{‡2}$ in HQET.

[23, 25, 26]. P. Gupta and A. Upadhyay [26] identified $D_J^*(3000)^0$ as a 2^3P_0 . J.-K. Chen [6] assigned the states $D_J(3000)^0$, $D_J^*(3000)^0$ and $D_2^*(3000)^0$ as 3^1S_0 , 3^3S_1 and 3^3P_2 respectively. S. Godfrey and K. Moats identified $D_J(3000)^0$ as 3^1S_0 state and $D_J^*(3000)^0$ as 3^3F_4 . To identify its nature, we expect some more experimental

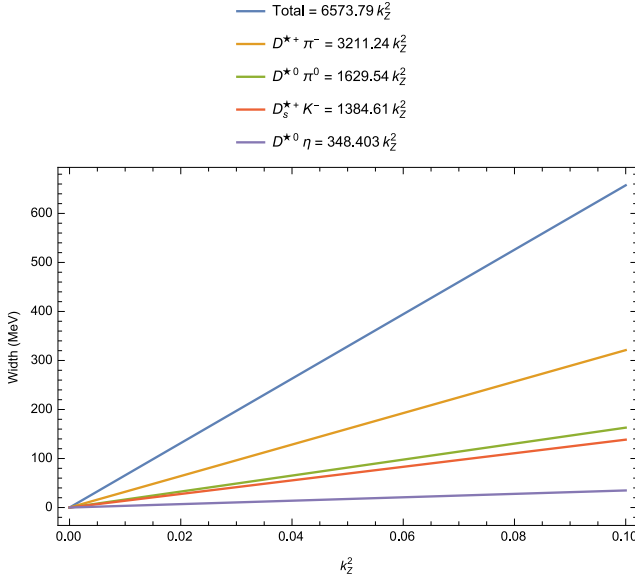


FIG. 19. Strong decay widths of 1^1F_3 (in MeV) nonstrange charmed meson state (lying on the Regge line 1^1S_0 in (J, M^2) plane) changing with the square of the coupling k_Z^2 in HQET.

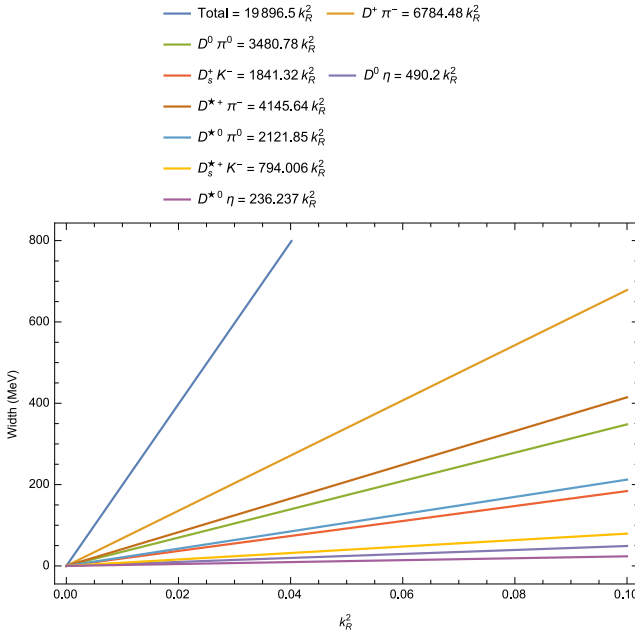


FIG. 20. Strong decay widths of 1^3F_4 (in MeV) nonstrange charmed meson state (lying on the Regge line 1^3S_1 in (J, M^2) plane) changing with the square of the coupling k_R^2 in HQET.

efforts in future.

Using these spin and parity assignments of experimentally observed D mesons, we construct the Regge trajectories in (J, M^2) and (n_r, M^2) planes. By fixing the slopes and intercepts of the Regge lines we estimate the masses of higher excited states 1^1D_2 , 1^3D_3 , 3^1S_0 , 3^3S_1 , 1^1F_3 , 1^3F_4 , 2^3D_3 , 3^3P_2 and 2^3F_4 of D mesons. Their

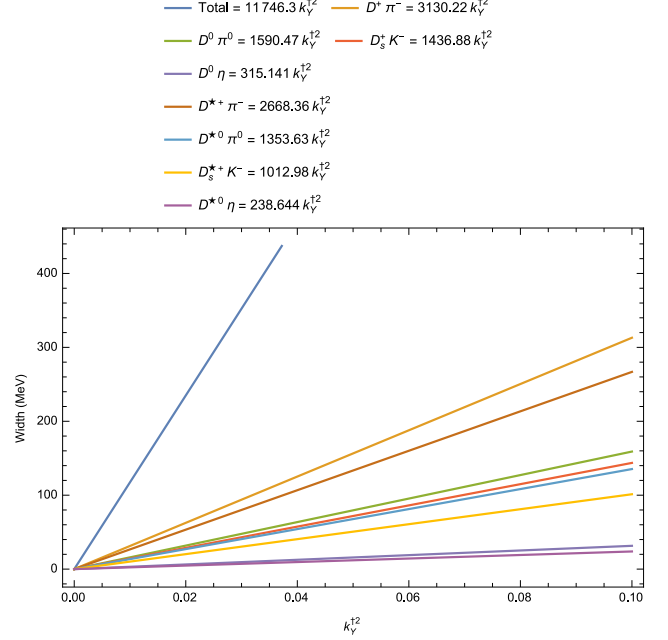


FIG. 21. Strong decay widths of 2^3D_3 (in MeV) nonstrange charmed meson state (lying on the Regge line 2^3S_1 in (J, M^2) plane) changing with the square of the coupling k_Y^{12} in HQET.

strong decays analysis conclude that the $D^{*+}\pi^-$ is dominant decay mode for 1^1D_2 , 3^1S_0 , 3^3S_1 , 1^1F_3 , 3^3P_2 states, and the decay mode $D^+\pi^-$ is dominant for 1^3D_3 , 1^3F_4 , 2^3D_3 , 2^3F_4 states. This study can help the experimentalists for searching these higher excited states in such decay modes. We would like to extend this scheme for the study of strong decays of excited strange charmed mesons in future.

-
- [1] R. Aaij *et al.* (LHCb Collaboration), Phys. Rev. D **94**, 072001 (2016).
[2] R. Aaij *et al.* (LHCb Collaboration), Phys. Rev. D **92**, 032002 (2015).
[3] R. Aaij *et al.* (LHCb Collaboration), JHEP **09**, 145 (2013).
[4] P. del Amo Sanchez *et al.* (BABAR Collaboration) Phys. Rev. D **82**, 111101(R) (2010).
[5] M. Tanabashi *et al.* (Particle Data Group), Phys. Rev. D **98**, 030001 (2018) and 2019 update.
[6] J.-K. Chena, Eur. Phys. J. C **648**, 78 (2018).
[7] V. Kher, N. Devlani, and A.K. Rai, Chin. Phys. C **41**,

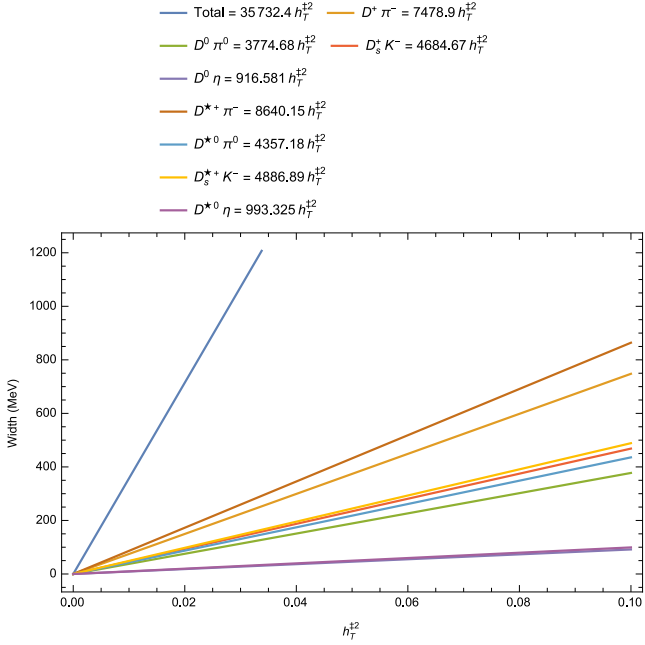


FIG. 22. Strong decay widths of 3^3P_2 (in MeV) nonstrange charmed meson state (lying on the Regge line 1^3P_2 in (n_r, M^2) plane) changing with the square of the coupling $h_T^{\pm 2}$ in HQET.

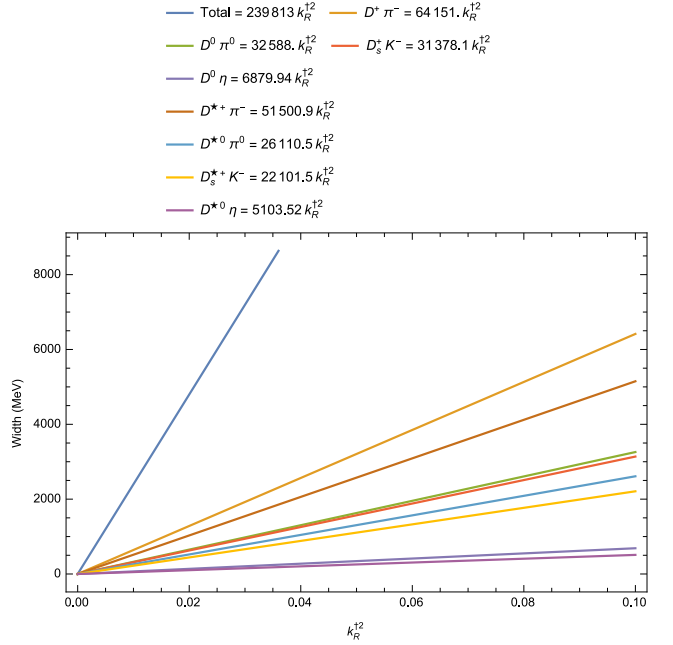


FIG. 23. Strong decay widths of 2^3F_4 (in MeV) nonstrange charmed meson state (lying on the Regge line 2^3S_1 in (n_r, M^2) plane) changing with the square of the coupling $k_R^{\pm 2}$ in HQET.

- 073101 (2017).
- [8] S. Godfrey and K. Moats, Phys. Rev. D **93**, 034035 (2016).
 - [9] Y. Sun, X. Liu, and T. Matsuki, Phys. Rev. D **88**, 094020 (2013).
 - [10] D.M. Li, P.F. Ji, and B. Ma, Eur. Phys. J. C **71**, 1582 (2011).
 - [11] D. Ebert, R.N. Faustov, and V.O. Galkin, Eur. Phys. J. C **66**, 197 (2010).
 - [12] M. Di Pierro and E. Eichten, Phys. Rev. D **64**, 114004 (2001).
 - [13] T.A. Lahde, C.J. Nyfalt, and D.O. Riska, Nucl. Phys. A **674**, 141 (2000).
 - [14] K. Cichy, M. Kalinowski, and M. Wagner, Phys. Rev. D, **94** 094503 (2016).
 - [15] X.-H. Zhong, Phys. Rev. D **82**, 114014 (2010).
 - [16] L.-Y. Xiao and X.-H. Zhong, Phys. Rev. D **90**, 074029 (2014).
 - [17] P. Colangelo, F. De Fazio, and R. Ferrandes, Phys. Lett. B **634**, 235 (2006).
 - [18] P. Colangelo, F. De Fazio, and S. Nicotri, Phys. Lett. B **642**, 48 (2006).
 - [19] P. Colangelo, F. De Fazio, S. Nicotri, and M. Rizzi, Phys. Rev. D **77**, 014012 (2008).
 - [20] P. Colangelo and F. De Fazio, Phys. Rev. D **81**, 094001 (2010).
 - [21] P. Colangelo, F. De Fazio, F. Giannuzzi, and S. Nicotri, Phys. Rev. D **86**, 054024 (2012).
 - [22] Z.G. Wang, Phys. Rev. D **83**, 014009 (2011).
 - [23] Z.G. Wang, Commun. Theor. Phys. **57**, 93 (2012).
 - [24] Z.G. Wang, Phys. Rev. D **88**, 114003 (2013).
 - [25] M. Batra and A. Upadhyay, Eur. Phys. J. C **75**, 319 (2015).
 - [26] P. Gupta and A. Upadhyay, Phys. Rev. D **97**, 014015 (2018).
 - [27] M. Neubert, Phys. Rep. **245**, 259 (1994).
 - [28] A. F. Falk, Nucl. Phys. B **378**, 79 (1992).
 - [29] A. F. Falk and M. E. Luke, Phys. Lett. B **292**, 119 (1992).
 - [30] R. Casalbuoni *et al.*, Phys. Rep. **281**, 145 (1997).
 - [31] S. Campanella, P. Colangelo, and F. De Fazio Phys. Rev. D **98**, 114028 (2018).
 - [32] R. Casalbuoni *et al.*, Phys. Lett. B **302**, 95 (1993); F. De Fazio, Phys. Rev. D **79**, 054015 (2009); Z. G. Wang, Eur. Phys. J. A **47**, 94 (2011); Z. G. He, X. R. Lu, J. Soto and Y. Zheng, Phys. Rev. D **83**, 054028 (2011); Z.G. Wang, Int. J. Theor. Phys. **51**, 1518 (2012); Mod. Phys. Lett. A **27**, 1250197 (2012).
 - [33] B. Singh *et al.* (PANDA Collaboration), Phys. Rev. D **95**, 032003 (2017); Eur. Phys. J. A **52**, 325 (2016); Nucl. Phys. A **954**, 323 (2016); Eur. Phys. J. A **51**, 107 (2015); J. Phys. G **46**, 045001 (2019).
 - [34] G. Barucca *et al.* *et al.* (PANDA Collaboration), Eur. Phys. J. A **55**, 42 (2019).
 - [35] P. Colangelo, F. De Fazio, G. Nardulli, N. Di Bartolomeo, and R. Gatto, Phys. Rev. D **52**, 6422 (1995).
 - [36] R. Casalbuoni, A. Deandrea, N. Di Bartolomeo, F. Feruglio, R. Gatto, and G. Nardulli, Phys. Rep. **281**, 145 (1997).
 - [37] Z. G. Wang and S. L. Wan, Phys. Rev. D **74**, 014017 (2006).
 - [38] Z. G. Wang, Nucl. Phys. A **796**, 61 (2007).
 - [39] P. Z. Huang, L. Zhang, and S. L. Zhu, Phys. Rev. D **81**, 094025 (2010).
 - [40] P. Avery *et al.* (CLEO Collaboration), Phys. Rev. D **41**, 774 (1990).
 - [41] S. Chekanov *et al.* (ZEUS Collaboration), Eur. Phys. J C **60**, 25 (2009).
 - [42] H. Abramowicz *et al.* (ZEUS Collaboration), Nucl.

- Phys. B **866**, 229 (2009).
- [43] B. Aubert *et al.* (*BABAR* Collaboration), Phys. Rev. D **79**, 112004 (2009).
- [44] T. Bergfeld *et al.* (*CLEO* Collaboration), Phys. Lett. B **340**, 194 (1994).
- [45] P.D. Collins, An introduction to Regge theory and high energy physics (Cambridge University Press, 1977).
- [46] S. Godfrey and J. Napolitano, Rev. Mod. Phys. D **66**, 1411 (1999).
- [47] P. del Amo Sanchez *et al.*, Phys. Rev. D **82**, 111101 (2010).
- [48] X.-H. Guo, K.-W. Wei, and X.-H. Wu, Phys. Rev. D **78**, 056005 (2008).
- [49] A. Zhang, Phys. Rev. D **72**, 017902 (2005).
- [50] D.-M. Li, B. Ma, Y.-X. Li, Q.-K. Yao, and H. Yu, Eur. Phys. J C **37**, 323 (2004).
- [51] M. M. Brisudova, L. Burakovsky, and T. Goldman, Phys. Rev. D **61**, 054013 (2000).